Institutionen för systemteknik
Department of Electrical Engineering

Examensarbete

Model-based turbocharger control - a common approach for SI and CI engines

Examensarbete utfört i Fordonssystem
vid Tekniska högskolan vid Linköpings universitet
av

Erik Lindén och David Elofsson

LiTH-ISY-EX--11/4487--SE

Linköping 2011

Linköpings universitet
TEKNISKA HÖGSKOLAN

Department of Electrical Engineering
Linköpings universitet
SE-581 83 Linköping, Sweden

Linköpings tekniska högskola
Linköpings universitet
581 83 Linköping

Model-based turbocharger control - a common approach for SI and CI engines

Examensarbete utfört i Fordonssystem
vid Tekniska högskolan i Linköping
av

Erik Lindén och David Elofsson

LiTH-ISY-EX--11/4487--SE

Handledare: **Oskar Leufvén**
ISY, Linköpings universitet
Andreas Thomasson
ISY, Linköpings universitet
Anders Larsson
Scania CV AB

Examinator: **Lars Eriksson**
ISY, Linköpings universitet

Linköping, 16 August, 2011

Avdelning, Institution
Division, Department

Division of Automatic Control
Department of Electrical Engineering
Linköpings universitet
SE-581 83 Linköping, Sweden

Datum
Date

2011-08-16

Språk
Language

☐ Svenska/Swedish
☒ Engelska/English
☐ _____

Rapporttyp
Report category

☐ Licentiatavhandling
☒ Examensarbete
☐ C-uppsats
☐ D-uppsats
☐ Övrig rapport
☐ _____

ISBN
__

ISRN
LiTH-ISY-EX--11/4487--SE

Serietitel och serienummer **ISSN**
Title of series, numbering __

URL för elektronisk version
http://www.vehicular.isy.liu.se/
http://www.ep.liu.se

Titel
Title

Modellbaserad turboreglering
- en ansats för både otto- och dieselmotorer

Model-based turbocharger control
- a common approach for SI and CI engines

Författare
Author

Erik Lindén och David Elofsson

Sammanfattning
Abstract

In this master's thesis, a turbine model and a common control structure for the turbocharger for SI and CI-engines is developed. To design the control structure, simulations are done on an existing diesel engine model with VGT. In order to be able to make simulations for engines with a wastegated turbine, the model is extended to include mass flow and turbine efficiency for that configuration. The developed model has a mean absolute relative error of 3.6 % for the turbine mass flow and 7.4 % for the turbine efficiency. The aim was to control the intake manifold pressure with good transients and to use the same control structure for VGT and wastegate. By using a common structure, development and calibration time can be reduced. The non-linearities have been reduced by using an inverted turbine model in the control structure, which consists of a PI-controller with feedforward. The controller can be tuned to give a fast response for CI engines and a slower response but with less overshoot for SI engines, which is preferable.

Nyckelord
Keywords

modeling, model-based control, non-linear control, turbocharged SI engine, turbocharged CI engine, wastegate, VGT

Abstract

In this master's thesis, a turbine model and a common control structure for the turbocharger for SI and CI-engines is developed. To design the control structure, simulations are done on an existing diesel engine model with VGT. In order to be able to make simulations for engines with a wastegated turbine, the model is extended to include mass flow and turbine efficiency for that configuration. The developed model has a mean absolute relative error of 3.6 % for the turbine mass flow and 7.4 % for the turbine efficiency. The aim was to control the intake manifold pressure with good transients and to use the same control structure for VGT and wastegate. By using a common structure, development and calibration time can be reduced. The non-linearities have been reduced by using an inverted turbine model in the control structure, which consists of a PI-controller with feedforward. The controller can be tuned to give a fast response for CI engines and a slower response but with less overshoot for SI engines, which is preferable.

Acknowledgments

It has been truly interesting to get the opportunity to make this project at the "heart" of Scania R&D, i.e. the Engine Performance Software. The task was comprehensive and included many different aspects of both physics and control theory. We are very pleased with the support that we got both from the university and from Scania. Thanks to our examiner, Associate Professor Lars Eriksson, for your support and ideas that helped us go into new directions when we were struggling. Our supervisors from the university, Oskar Leufvén and Andreas Thomasson are acknowledged for guiding us in the right direction and for quick and good responses to our many questions. Special thanks goes to Anders Larsson, supervisor at Scania, for all interesting discussions we have had. You always had good ideas on how to progress and how to overcome obstacles that was rarely thought of before. The group NESE at Scania is acknowledge for your input and support during the project. It was a pleasure to work with all of you for one semester.

Erik Lindén
Linköping, August 2011

David Elofsson
Linköping, August 2011

Contents

Chapter 1

Introduction

In this chapter, an introduction to the thesis work is given, with background and problem formulation. Furthermore, the expected results of the work are stated.

1.1 Background

The components of the engine that ensure that the engine gets the correct amount of oxygen for combustion are called the gas flow system. The system consists of a number of components, actuators and sensors; e.g. air filter, turbo, intercooler, throttle, exhaust gas recirculation (EGR) system, intake manifold, exhaust manifold, exhaust system, etc. To meet future requirements in terms of performance, emissions and fuel consumption, it is necessary to control the gas flow system through control of the EGR system and turbocharger (see [18]). The turbocharger can be either a variable geometry turbocharger (VGT) or a wastegate turbocharger. Models of turbocharged compression ignition (CI) and spark ignition (SI) engines are increasingly being used to design and test control strategies, but control-oriented modeling of the turbocharger has received limited attention, even if the turbocharger sub-model is a critical part of the overall model (see [11]). In the area of gas flow control, a lot of attention is given to coordinated control of VGT and EGR (see Section 2). Other configurations are however possible, for example a configuration with VGT in combination with wastegate for better temperature control of the exhaust gases. In order to further reduce emissions from CI engines, the use of particle filters is increasing. Particle filters demand high exhaust gas temperatures, which is commonly solved with a separate burner, but as high exhaust gas temperatures as possible from the engine combustion would be preferable. Since the temperature decreases when gases flow through the turbine, the optimal solution when no inlet gas compression is needed, would be for the exhaust gases to bypass the turbine. Even if the VGT is fully opened, some turbine work is extracted, and a wastegate would make it possible to bypass more exhaust gases.

1.2 Purpose and Goal

The aim of the Master's thesis is to extend an existing CI engine model (presented in [18]) with a wastegate turbo block and to develop a model-based controller to meet future requirements for both SI and CI engines. The engine model is only validated for CI engines, but the gas-flow equations are the same for CI and SI engines, and the aim is to develop a control algorithm independent of whether the engine is compression or spark ignited. The main goals are:

1. Build a model of the wastegate turbocharger, which is missing in the existing engine model. The model should then be the basis for controller design.

2. Study and design a model-based control algorithm for the turbocharger. The aim is to develop a control algorithm that controls the turbocharger speed, with reference values in intake manifold pressure, with the turbine actuator (wastegate valve or VGT actuator).

1.3 Problem Formulation

Truck engines come in several different configurations, where both SI and CI engines use different solutions for the turbo charging system, and with or without EGR. To meet emission requirements, the combination VGT and EGR is common on CI engines, but on SI engines the VGT cannot be used because of too hot exhaust gases. On SI engines it is common to use a wastegate turbo instead, which is usually also a cheaper and more robust solution than the VGT.

In the industry there are possible cost savings if models and control algorithms can be developed and reused for different engines and configurations. This project aims at developing a turbine model that could be used to design control algorithms for engines with both VGT and wastegate. The model should also be useable for other configurations. By viewing the VGT as a wastegate turbine with closed wastegate valve and with varying characteristics (altered by the VGT actuator), a single model for the two different turbines could be developed. The controller will be developed to control only the turbine actuator, which makes it possible to combine the controller with e.g. an engine configuration without EGR.

Controlling the system is a real challenge because there are strong multiple cross couplings between control signals and output signals. The system is highly nonlinear, and shows non-minimum phase behavior in certain operating points.

1.4 Expected Results

In this section, the expected results are presented.

1. General goals
   - Develop a control algorithm that can be run in a test cell.
   - Use the same control algorithm (approximately) for SI and CI engines with wastegate and VGT.
2. Model goals
   - A maximum absolute relative error of 10 % for the states[1] n_t, p_{im}, $\dot{m}_{ei}$, x_{egr}, λ_O.
3. Controller goals
   - The control algorithm should have a better transient behavior in torque than the current algorithm.
     - Reach 70 % of requested torque in less than 4 s at 1200 rpm.
   - For SI engine: Maximum 5 % overshoot in p_{im} (since $\lambda = 1$ in SI engines, overshoot in intake manifold pressure can lead to an overshoot in torque).

[1] n_t = turbocharger rotational speed, p_{im} = intake manifold pressure, $\dot{m}_{ei}$ = mass flow into the cylinders, x_{egr} = EGR-fraction, λ_O = oxygen-to-fuel ratio. See Table 3.1.

Chapter 2

Related research

In this chapter, related research within the fields of modeling and control is presented. This work is furthermore positioned in relation to what has already been done.

2.1 Modeling

The basis for this project is an engine model developed by Johan Wahlström, see [18]. It is a mean value model of a diesel engine with intake throttle, VGT and EGR. The existing model does not include a block for the wastegate, but that will be included in this work. It is stated in [10], that there are few works that deal with turbocharged SI engine control with a model that includes throttle, wastegate valve and EGR valve. In that paper a model and a nonlinear controller have been developed.

A Simulink model of a turbocharged SI engine is presented in [2]. This model consists of a block that represents both turbine and wastegate. Another example in the same book shows a CI engine with VGT and EGR. Nothing is mentioned about the CI engine with wastegate, but it is likely that the model will be similar to the SI engine with the same setup. According to [3] many components can be found on both SI and CI engines, and a component based approach is therefore good for the re-usage of models. In [3] there is an example of a Simulink model for a turbocharged CI engine with VGT and EGR. The methodology used is to divide the system into components and then use rules of physics and thermodynamics.

The turbocharged SI engine can be seen as a multiple input, multiple output (MIMO) system, see [10]. However, when designing the controller, the system will be seen as a multiple input, single output (MISO) system, where the turbine actuator control signal is the single output. In [10], the control signal to the wastegate is a pulse-width modulation (PWM) signal, which is the case for the Scania engines as well.

Turbocharger performance maps are typically presented in table form, but in order to be useful in engine simulation models, this can be insufficient, see [11]. Curve fitting methods for compressor and turbine characteristics are presented

in [11], and according to [8] the turbine efficiency is the most difficult to model. The turbocharger is typically modeled using performance maps provided by the manufacturer, but these are insufficient in describing performance in the low and medium speed regions. Those regions, which are important for emissions, are typically modeled by simply extrapolating the maps ([8]).

2.2 Controller design

Coordinated control of EGR and VGT for lower emissions is relatively well described in publications, since a VGT provides flexible control of turbine speed and gas flow restriction. Among the first to investigate and present the benefits of coordinated EGR and VGT control, as opposed to the traditionally used SISO controllers, is M. van Nieuwstadt et al. in [12]. A thorough analysis and description of modeling of a diesel engine and proposal of a robust airpath control is given in [8]. In [6], a robust control Lyapunov function is developed using input-output linearization. The development is based on a reduced order diesel engine. Another combined VGT-EGR control is proposed in [13], who also use Lyapunov theory to prove robustness. Lyapunov theory is also used in [21], where a controller based on feedback linearization with integral action is proposed to control the oxygen-to-fuel ratio and EGR-fraction. A fuzzy logic controller is presented in [15] and [14], and the aim in these papers is air-to-fuel ratio control. Models for VGT and EGR together with investigations of control strategies are presented in several papers by L. Eriksson and J. Wahlström, see e.g. [18], [17] and [20].

There are however engine configurations with wastegated turbine instead of VGT, since it is cheaper and more robust, and also configurations without EGR. A model and control approach, where solutions can be reused for different configurations, would therefore be desirable. MISO controllers, where single actuators are controlled with e.g. other actuator positions as input, would give that opportunity. In this work a controller for wastegate actuator and VGT actuator control is proposed. Mathematical models of engines are very complex, and even if control with feedback allows for some modeling error it is still a 'leap of faith' to implement a controller on such a complex system. Model-based control demands simplified models, which further introduces uncertainty, and the robustness of the controller is hence very important. An H_∞ loop-shaping based control to optimize robustness for the airpath control in a CI engine is proposed in [7].

Different approaches to model-based control of diesel and SI engines have been proposed in several publications. In [1], a component based model for the gas flow systems in turbocharged SI engines is developed and used for an observer based feedforward control of the air-fuel ratio λ, with transient deviations less than 7 % in rapid throttle transients. The proposed controller also uses a slower PI feedback loop for λ, to improve stationary errors. In [16], a structure with PID controllers and selectors for coordinated control of EGR and VGT-position is proposed. The performance variables chosen are oxygen/fuel ratio, λ_O, and intake manifold EGR fraction, x_{egr}. The choice of λ_O as performance variable, instead of λ, is argued to better handle the fact that there is oxygen left in the

recirculated exhaust gases. Since both x_{egr} and λ_O depend in complicated ways of the actuation of both EGR and VGT, as shown in [22], it is argued to be necessary to have coordinated control of the EGR and VGT to reach emission and smoke limits, and [12] shows that better performance in regions with low speed/low load is possible with a multivariable controller rather than with SISO techniques. In [16], λ_O is controlled by the EGR-valve and x_{egr} is controlled by the VGT-position, since it handles a sign reversal in the system from VGT to λ_O.

One paper that deals with wastegate control is [9], where a control approach for a turbocharged SI engine equipped with wastegate and electronic throttle is proposed. The controller is based on a non-linear mean value model for the system, which is linearized in multiple operating points. A gain scheduled, decentralized controller is designed to control intake manifold pressure and boost pressure, and a multivariable control approach is further considered. There is however no EGR on that system, which is dealt with in this work.

In [19], a non-linear compensator in an inner loop is used to handle non-linear effects. The compensator is a non-linear state dependent input transformation, and an outer loop with PID controllers and selectors similar to the controller in [16] is used to stabilize the system. The compensator is developed by inverting the models for EGR flow and turbine flow, which is also the proposed approach in [6] where similar models for EGR flow and turbine flow are inverted. This approach is shown to reduce EGR-errors but increase pumping losses compared to [16].

In [16], λ_O and x_{egr} are chosen as main feedback variables, and in [19] the feedback variables are EGR flow, W_{egr}, and exhaust manifold pressure, p_{em}, in the outer PID feedback loop.

The controller design approach in this work, is to use the turbocharger speed n_t as feedback variable in a linear controller, with wastegate actuator u_{wg} or VGT actuator u_{vgt} as control signals. To be able to use a linear controller, a linearization of the input and output signals is needed.

Chapter 3

System description

In this chapter a brief description of the system is given. An overview of the system is given in Figure 3.1, showing control volumes, gas flows and flow restrictions in the engine. The system overview shows all gas flow components, even if most engine configurations does not have all those. For example, the combination wastegate and VGT is rare, and also EGR with wastegate. In [22], a comprehensive analysis and description of the gas flow system and its properties in a diesel engine with VGT and EGR is given, and the interested reader is recommended to take part of these results. Among the most important results for this study are sign reversals in the channels $u_{vgt} \to \lambda_O$, $u_{egr} \to \lambda_O$ and $u_{vgt} \to x_{egr}$, which all have negative DC gains in large operating regions. Other important results are non-minimum phase behaviours, strong cross-couplings between signals and varying response times.

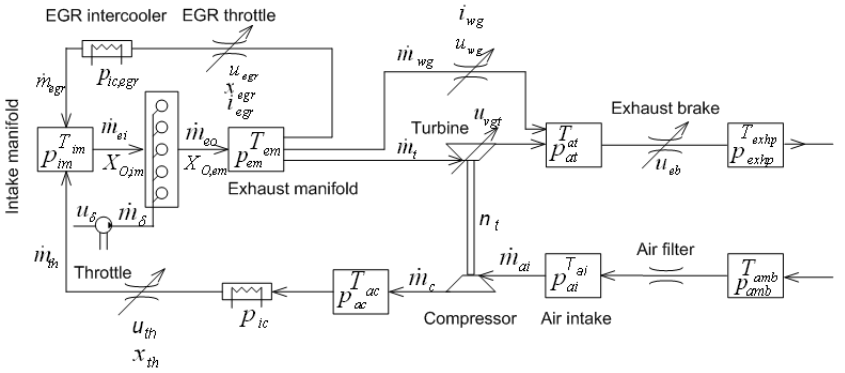

Figure 3.1. Model structure of an engine with both a VGT and a wastegate, the structure also contains an EGR-system. All variables are explained in Table 3.1

.

The following tables show variables, signals, constants and subscripts used in the report.

Table 3.1. Variables

Variable	Description	Unit
i	Current	[A]
n	Rotational speed	[rpm]
ω	Angular velocity	[rad/s]
p	Pressure	[Pa]
T	Temperature	[K]
$\dot{m}$	Mass flow	[kg/s]
X_O	Oxygen concentration	[-]
λ_O	Oxygen/fuel ratio	[-]
x	Actuator position	[mm or %]
M	Torque	[Nm]
P	Power	[W]

Table 3.2. Control signals

Control signal	Description	Unit
u_δ	Fuel injection control signal	mg/cycle
u_{egr}	EGR control signal. 0 - closed, 100 - open	%
u_{eb}	Exhaust brake control signal. 0 - closed, 100 - open	%
u_{th}	Intake throttle control signal. 0 - closed, 100 - open	%
u_{wg}	Wastegate control signal. 0 - closed, 100 - open	%
u_{vgt}	VGT control signal. 0 - closed, 100 - open	%

Table 3.3. Constants

Constant	Description	Unit
γ	ratio of specific heats	[-]
c_p	Specific heat capacity at constant pressure	$[\mathrm{J/(kg \cdot K)}]$
c_v	Specific heat capacity at constant volume	$[\mathrm{J/(kg \cdot K)}]$
J	Inertia	$[\mathrm{kg \cdot m^2}]$
R	Gas constant	$[\mathrm{J/(kg \cdot K)}]$

Table 3.4. Subscripts

Subscript	Description
a	air
e	exhaust
amb	ambient
t	turbine
c	compressor
egr	EGR
wg	wastegate
vgt	VGT
$corr$	corrected quantity
ai	air intake
bc	before compressor
ac	after compressor
bt	before turbine
at	after turbine
em	exhaust manifold
im	intake manifold
ic	intercooler
$exhp$	exhaust pipe
δ	fuel injection
ei	engine intake
eo	engine outlet
th	throttle
m	mechanical

Chapter 4

Turbocharging

In this chapter, the concept of turbocharging is described, as well as some definitions for later use in the report.

4.1 Performance

In turbine and compressor maps, corrected quantities are normally used in order to make the model more general and work for different temperature and pressure conditions.

4.1.1 Compressor maps

The compressor map consists of four performance variables: corrected mass flow, pressure ratio, corrected shaft speed and compressor (adiabatic) efficiency. Corrected mass flow is used to make the measurements applicable for varying conditions. The correction is made with the temperature and pressure before the compressor, and reference values for the same. The reference values are provided from the manufacturer, together with the map. The corrected mass flow is given by

$$\dot{m}_{c,corr} = \dot{m}_c \frac{\sqrt{\frac{T_{bc}}{T_{c,ref}}}}{\frac{p_{bc}}{p_{c,ref}}} \tag{4.1}$$

and the included variables are explained in Table 3.1. The pressure ratio is given by the quotient between pressure after and before the compressor

$$\Pi_c = \frac{p_{ac}}{p_{bc}} \tag{4.2}$$

and the corrected shaft speed is given by

$$n_{c,corr} = n_t \frac{1}{\sqrt{\frac{T_{bc}}{T_{c,ref}}}} \tag{4.3}$$

The compressor adiabatic efficiency is given by

$$\eta_c = \frac{P_{c,ideal}}{P_c} = \frac{\left(\frac{p_{ac}}{p_{bc}}\right)^{\frac{\gamma_a - 1}{\gamma_a}} - 1}{\frac{T_{ac}}{T_{bc}} - 1} \tag{4.4}$$

where $P_{c,ideal}$ is the power given by an ideal adiabatic process (process with no net heat transfer).

The compressor power is given by

$$P_c = \dot{m}_c c_{p,c}(T_{ac} - T_{bc}) \tag{4.5}$$

or by

$$P_c = \frac{\dot{m}_c c_{p,c} T_{bc}}{\eta_c}\left[\Pi_c^{\frac{\gamma_a - 1}{\gamma_a}} - 1\right] \tag{4.6}$$

4.1.2 Turbine maps

The turbine map also consists of four performance variables: corrected mass flow, expansion ratio, corrected shaft speed and turbine (adiabatic) efficiency. Additionally, two more variables are sometimes defined for the turbine: turbine flow parameter and turbine speed parameter. The corrected turbine mass flow is given by

$$\dot{m}_{t,corr} = \dot{m}_t \frac{\sqrt{\frac{T_{em}}{T_{t,ref}}}}{\frac{p_{em}}{p_{t,ref}}} \tag{4.7}$$

and the corrected shaft speed by

$$n_{t,corr} = n_t \sqrt{\frac{T_{t,ref}}{T_{em}}} \tag{4.8}$$

but it is common to neglect the nominal states $T_{t,ref}$ and $p_{t,ref}$ and use the turbine flow parameter (TFP) and turbine speed parameter (TSP) instead

$$TFP = \dot{m}_t \frac{\sqrt{T_{em}}}{p_{em}} \tag{4.9}$$

$$TSP = n_t \frac{1}{\sqrt{T_{em}}} \tag{4.10}$$

The turbine pressure ratio is given by

$$\Pi_t = \frac{p_{at}}{p_{bt}} \tag{4.11}$$

but in the turbine map, the turbine expansion ratio is normally used

$$\frac{1}{\Pi_t} = \frac{p_{bt}}{p_{at}} \tag{4.12}$$

The turbine adiabatic efficiency is given by the ratio between the power given by an ideal adiabatic process and the actual turbine power

$$\eta_t = \frac{P_t}{P_{t,ideal}} = \frac{1 - \frac{T_{at}}{T_{bt}}}{1 - \left(\frac{p_{at}}{p_{bt}}\right)^{\frac{\gamma_e - 1}{\gamma_e}}} \tag{4.13}$$

but since the turbine power

$$P_t = \dot{m}_t c_{p,t}(T_{bt} - T_{at}) \tag{4.14}$$

is hard to estimate accurately due to large heat transfers from the hot exhaust gases, a more common way to describe the turbine efficiency is the ratio between compressor power and the ideal adiabatic process

$$\eta_{tm} = \eta_t \cdot \eta_m = \frac{\dot{m}_c c_{p,c}(T_{ac} - T_{bc})}{\dot{m}_t c_{p,t} T_{bt}\left(1 - \left(\frac{p_{at}}{p_{bt}}\right)^{\frac{\gamma_e - 1}{\gamma_e}}\right)} \tag{4.15}$$

where η_m is the mechanical efficiency introduced by the shaft friction.

4.2 Turbo dynamics

The compressor and turbine power are connected with a shaft. The connection introduces some losses, defined as the mechanical efficiency η_m.

At steady state the connection between compressor and turbine power is

$$P_c = \eta_m P_t \tag{4.16}$$

During transients the dynamic response is modeled using Newton's second law:

$$\frac{d\omega}{dt} = \frac{1}{J_t}\left(\frac{P_t}{\omega}\eta_m - \frac{P_c}{\omega}\right) \tag{4.17}$$

or

$$\frac{d\omega}{dt} = \frac{1}{J_t}\left(\frac{P_t}{\omega} - \frac{P_c}{\omega} - M_{fric}(\omega)\right) \tag{4.18}$$

where $M_{fric}(\omega_{tb})$ is the friction torque, usually modeled as a quadratic function in rotational speed, and ω is the angular velocity ($\omega = 2\pi n$) ([2]).

Chapter 5

Modeling

In this chapter the modeling of the wastegated turbocharger is described. The model consists of two submodels: turbine mass flow and turbine efficiency. Firstly the test data that has been used is described, followed by each submodel.

5.1 Test data

The model is based on two test data sets that have been collected in a test cell at Scania CV. The engine had a fixed geometry turbine with a wastegate and an intake throttle. The intake throttle was fully opened and no EGR was used. During measurements, the test points were all stationary. The engine speed, n_e, has five different values and for each value there are five ascending values of M_e except for the third M_e-cycle, where the last value of M_e is missing. This makes 24 combinations of n_e and M_e. The first five of these are removed though since M_e is rising continuously instead of ascending in intervals. For each of these 19 combinations, a u_{wg} cycle is run, from 0 to 65 percent pwm-signal. The first test data set is used for estimation of the model parameters and is further presented in Figure 5.1. Since the test data sets are stationary, the model of the wastegated turbocharger is a static model. The second test data set is used for validation.

5.2 Turbine mass flow

The flow through the wastegated turbine can be modeled as two separate flows: one through the turbine and one through the wastegate. The equations that have been used in the model will now be presented, followed by the parametrization and validation.

5.2.1 Equations

Firstly, equations for the flow through a turbine will be presented and secondly a methodology will be presented to determine the flow when a wastegate is included

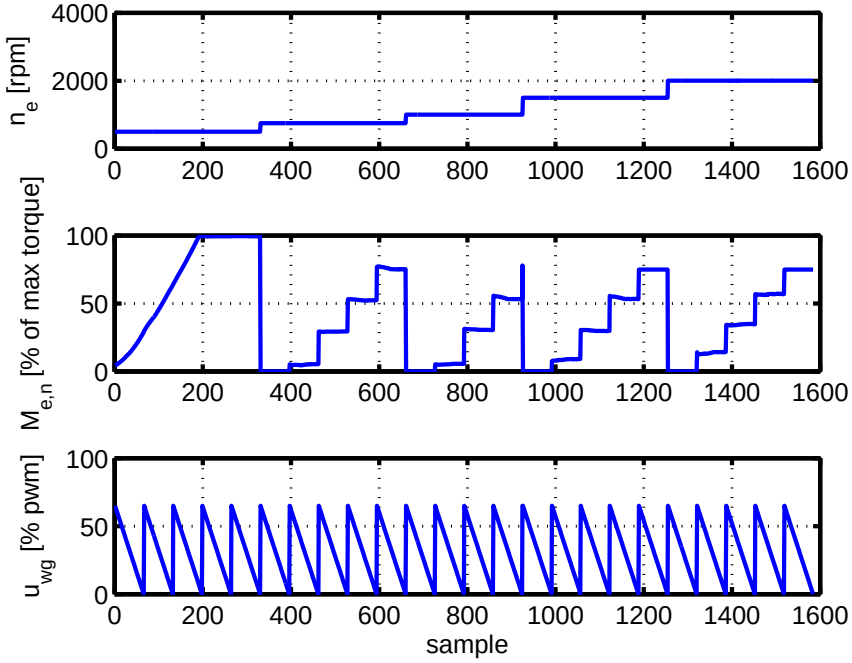

Figure 5.1. This figure shows three of the signals in test data set one, used to estimate parameters of the model. The plot in the top of the figure shows the engine speed, the middle shows the nominal torque as a percentage of maximum torque and the bottom shows the pwm-signal to the wastegate. They are all plotted against sample number for the stationary data set points.

in the model.

The turbine pressure ratio Π_t is defined as (4.11). A standard model for compressible flow through a restriction (see e.g. [2]), can be applied to model the turbine flow

$$\dot{m} = \frac{p_{em}}{\sqrt{R_e T_{em}}} \cdot A_{eff} \cdot \underbrace{\Psi\left(\frac{p_{at}}{p_{em}}\right)}_{\Psi(\Pi)} \tag{5.1}$$

$$\Psi(\Pi) = \begin{cases} \sqrt{\frac{2\gamma}{\gamma-1}\left(\Pi^{\frac{2}{\gamma}} - \Pi^{\frac{\gamma+1}{\gamma}}\right)} & \text{if } \Pi > \left(\frac{2}{\gamma+1}\right)^{\frac{\gamma}{\gamma-1}}, \\ \sqrt{\frac{2\gamma}{\gamma-1}\left(\left(\frac{2}{\gamma+1}\right)^{\frac{2}{\gamma-1}} - \left(\frac{2}{\gamma+1}\right)^{\frac{\gamma+1}{\gamma-1}}\right)} & \text{otherwise} \end{cases} \tag{5.2}$$

where A_{eff} is the effective turbine area and R_e is the ideal gas constant for exhaust

gas.

The gas in the turbine is accelerated both in the stator (inlet and volute) and in the rotor (turbine wheel). If assuming that half the expansion will take place in the stator and the other half in the rotor, the flow through the turbine can be described by (5.1) and (5.2) if $\sqrt{\Pi_t}$ is inserted in (5.2), see [3]. It has also been found in [3] that the flow can be well described by a simpler non physical model

$$\dot{m}_{t,corr} = c_0\sqrt{1-\Pi^k} \tag{5.3}$$

where c_0 and k are tuning parameters.

The model (5.3) will be used because a simpler model is easier to simulate and it is also more appropriate for the choice of controller in this work, see Section 6. When the wastegate is closed, all the gas flows through the turbine. From the datapoins of the flow through the engine for these pwm-signals, the corrected mass flow can be calculated using (4.7). Equation 5.3 can then be used to model the flow.

The total flow through the wastegated turbine can be written as a sum of the turbine and the wastegate flow, leading to

$$\dot{m}_{wg} = \dot{m}_{tot} - \dot{m}_t \tag{5.4}$$

The flow through the wastegate can be modeled using the equations for compressible flow (5.1) and (5.2). The model for the turbine flow (5.3), gives a corrected mass flow and therefore the inverse of (4.7) is used to get $\dot{m}_t$. This leads to the equation

$$\frac{p_{em}}{\sqrt{RT_{em}}}A_{wg}\Psi(\Pi_t) = \dot{m}_{eo} - \frac{(p_{em}/p_{ref})}{\sqrt{T_{em}/T_{ref}}}c_0\sqrt{1-\Pi^k} \tag{5.5}$$

Solving (5.5) for A_{wg} gives the following expression:

$$A_{wg} = \left(\dot{m}_{eo}\frac{\sqrt{T_{em}}}{p_{em}} - \frac{(1/p_{ref})}{\sqrt{1/T_{ref}}}c_0\sqrt{1-\Pi^k}\right)\frac{\sqrt{R}}{\Psi(\Pi_t)} \tag{5.6}$$

By making use of (5.6) the turbine flow can be determined using (5.1).

5.2.2 Parametrization

The values of the parameters c and k in (5.3) are calculated by solving a non-linear least squares problem. The resulting model plotted against the data samples is seen in Figure 5.2. The model shows a good fit, with a mean absolute relative error of 4.9 %.

The tricky part for the flow through the wastegate is to find a model for the effective area, A_{wg}, of the wastegate. It is obvious that the area depends on u_{wg} since that is the control signal for the actuator, but there might be other parameters that also influence, e.g. Π_t. The expansion ratio influences the behavior of the actuator and can make it open even if u_{wg} is zero.

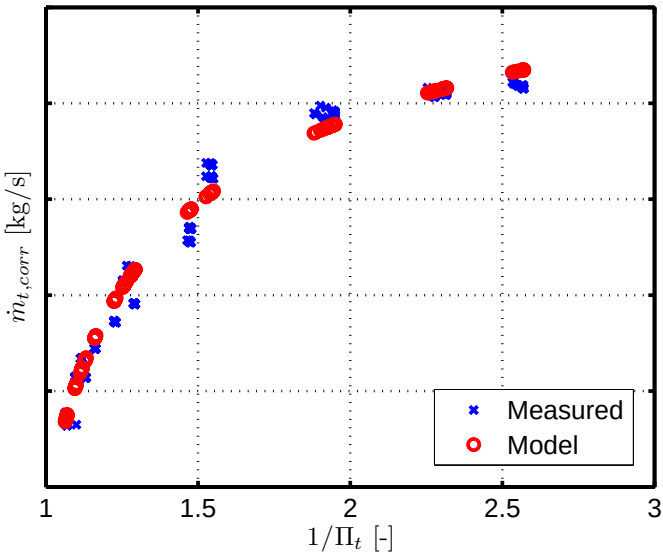

Figure 5.2. The non-physical model for the corrected turbine massflow (5.3) when the wastegate is closed, plotted against the measured values. The model shows a good fit, with a mean absolute relative error of 4.9 %.

In Figure 5.3 it can be seen that the area seems to be constant for $u_{wg} < 33$ % and for $u_{wg} > 33$ % it is increasing and could be described by a second order polynomial. It can also be seen that a greater area gives a lower expansion ratio. However, there is a dependence between these two variables. When the wastegate goes from open to closed, the area decreases which means p_{em} increases and therefore the expansion ratio also increases. It has been found that when knowing n_e and M_e, A_{wg} can be described as a function of only u_{wg}.

For each wastegate cycle, when u_{wg} goes from 0 to 65 % and for a specific n_e and M_e, A_{wg} can be modeled as

$$A_{wg} = max\Big(d_{A0}, d_{A1}u_{wg}^2 + d_{A2}u_{wg} + d_{A3}\Big) \tag{5.7}$$

where d_{A0}, d_{A1}, d_{A2} and d_{A3} are tuning parameters. All these parameters are calculated by solving a non-linear least squares problem. For the missing set, see Section 5.1, the parameters are an average of the surrounding values. When implementing the model in Simulink, look-up tables are used for these parameters with engine speed and torque as input.

The model is working well for this engine setup. When EGR is used a problem arises though. With EGR, no unique value of Π_t can be calculated for a certain combination of n_e and M_e and since the parameters for the model of A_{wg} are selected only based on that combination it might not be accurate. For a better model, the choice of parameters should be based on the value of Π_t.

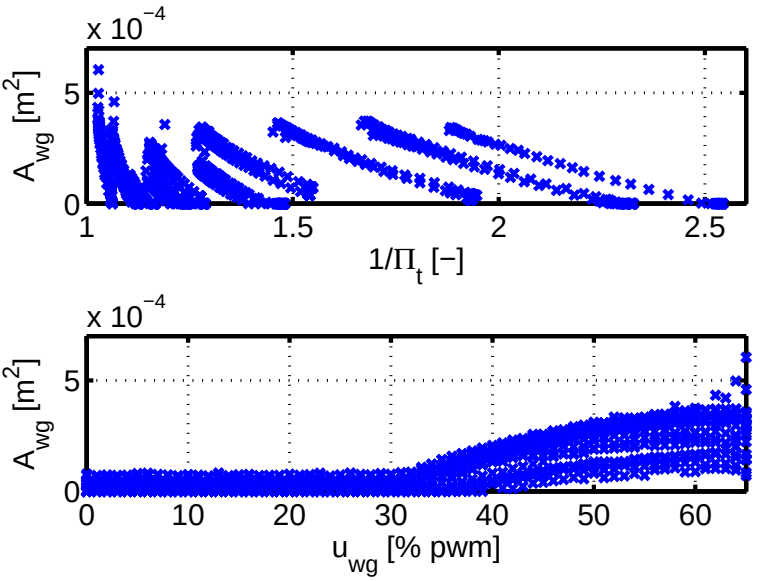

Figure 5.3. A_{wg} calculated with (5.6) using measured data. In the upper plot it can be seen that for one wastegate cycle, a smaller area gives a greater expansion ratio. In the lower plot it can be seen that the area seems to be constant for $u_{wg} < 33$ % and for $u_{wg} > 33$ % it is increasing and could be described by a second order polynomial.

5.2.3 Validation

Data set two has been used to validate the model for the total flow through the wastegate and the turbine. In Figure 5.4, it can be seen that the fit between the modeled flow and the measured flow is good. The mean absolute relative error is 3.6 %.

Another way to validate the model would have been to compare the turbine mass flow from the model with a turbine map. However, the turbine maps that were available for this work were constructed under unreasonable circumstances in a dynamometer and therefore it was better to validate against another data set.

5.3 Turbine efficiency

In this section the equations that have been used in the model for turbine efficiency will be presented, followed by the parametrization and validation.

5.3.1 Equations

The turbine power is defined as (4.14). If the conditions were ideal the turbine power would be

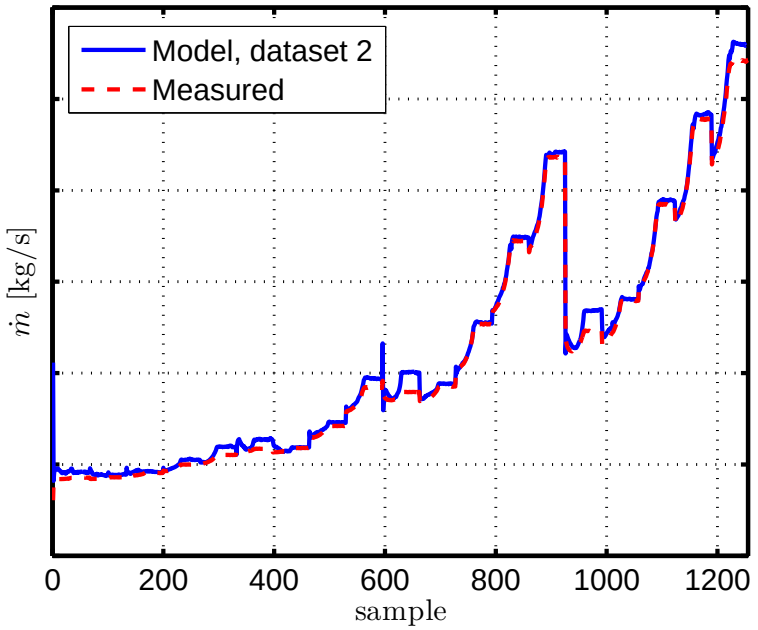

Figure 5.4. The output from the model of the total flow from the wastegate and the turbine when using data set two as input is plotted against the measured values of W_{ai} for the same data set. The mean absolute relative error is 3.6 %, meaning that the fit is good.

$$P_{t,ideal} = \dot{m}_t c_{pe} T_{em} \left(1 - \Pi_t^{1-\frac{1}{\gamma_e}}\right) \tag{5.8}$$

The turbine efficiency is defined as (4.13). The major issue with this equation is that it does not include temperature drops between T_{em} and T_{at} due to heat losses. In [2], the turbine efficiency is modeled as

$$\eta_t(BSR) = \eta_{tmax}\left(1 - \left(\frac{BSR - BSR_{opt}}{BSR_{opt}}\right)^2\right) \tag{5.9}$$

where BSR is defined as

$$BSR = \frac{\omega_t R_t}{\sqrt{2c_{pe}T_{em}\left(1 - \Pi_t^{\frac{\gamma_e - 1}{\gamma_e}}\right)}} \tag{5.10}$$

and tuning parameters are η_{tmax} and BSR_{opt}.

An alternative turbine efficiency used in [18] (see also p. 138 in [2]) is

$$\eta_{tm} = \eta_t \cdot \eta_m = \frac{\dot{m}_c c_{p,c}(T_{ac} - T_{bc})}{\dot{m}_t c_{p,t} T_{em}\left(1 - \left(\frac{p_{at}}{p_{em}}\right)^{\frac{\gamma_e - 1}{\gamma_e}}\right)} \tag{5.11}$$

where η_m is the mechanical efficiency from the turbine to the compressor (they are connected through a shaft). In this equation, the temperature difference T_{em} - T_{at} is not used. The expression utilizes that, for stationary operation,

$$P_t \eta_m = P_c \tag{5.12}$$

and the individual parts η_m and P_t does not have to be modeled separately. The product is modeled as

$$P_t \eta_m = \eta_{tm} P_{t,ideal} = \eta_{tm} \dot{m}_t c_{pe} T_{em} \left(1 - \Pi_t^{1-\frac{1}{\gamma_e}}\right) \tag{5.13}$$

In [18], η_{tm} is modeled as a function of the blade speed ratio, BSR, turbine speed, ω_t and the VGT actuator position, $\tilde{u}_{vgt}$:

$$\eta_{tm} = \eta_{tm,BSR}(BSR) \cdot \eta_{tm,\omega_t}(\omega_t) \cdot \eta_{tm,\tilde{u}_{vgt}}(\tilde{u}_{vgt}) \tag{5.14}$$

where

$$\eta_{tm,BSR}(BSR) = 1 - b_{BSR}\left(BSR^2 - BSR_{opt}^2\right)^2 \tag{5.15}$$

$$\eta_{tm,\omega_t}(\omega_t) = \begin{cases} 1 - b_{\omega t1}\omega_t & \text{if } \omega_t \leq \omega_{t,lim}, \\ 1 - b_{\omega t1}\omega_{t,lim} - b_{\omega t2}(\omega_t - \omega_{t,lim}) & \text{if } \omega_t > \omega_{t,lim} \end{cases} \tag{5.16}$$

where BSR is defined in (5.10). Tuning parameters are b_{BSR}, BSR_{opt}, b_{wt1}, b_{wt2} and $w_{t,lim}$. The value of $\eta_{tm,\tilde{u}_{vgt}}(\tilde{u}_{vgt})$ is set to one, since the model does not contain a VGT.

5.3.2 Parametrization

In order to find a good model for the turbine efficiency, both model 1, (5.9), and model 2, (5.14), are evaluated and the one that gives least error is chosen. The values of the parameters are calculated by solving a non-linear least squares problem. For model 2, it will be modeled in two steps, first with only the first factor and secondly with the first two factors. Since there is no VGT the third factor is set to one in both cases. The resulting models are plotted against the measured values in Figure 5.5. Model 1 gives a mean absolute relative error of 7.4 % and the corresponding value for model 2, i.e. the first factor in (5.14), is 9.4 %. If both factors are used in model 2, the result is slightly better than model 1, a mean absolute relative error of 7.1 %. However, since the complexity is lower for model 1 with similar behavior, model 1 is chosen.

5.3.3 Validation

The best way to validate the model for the turbine efficiency, (5.9), would be to use the turbine map. As mentioned in Section 5.2.3, the turbine maps that were available for this work were constructed under unreasonable circumstances compared to the conditions that the measured data was collected in. Therefore data set 2 has been used for validation, see Figure 5.6. The mean absolute relative error is 7.4 %.

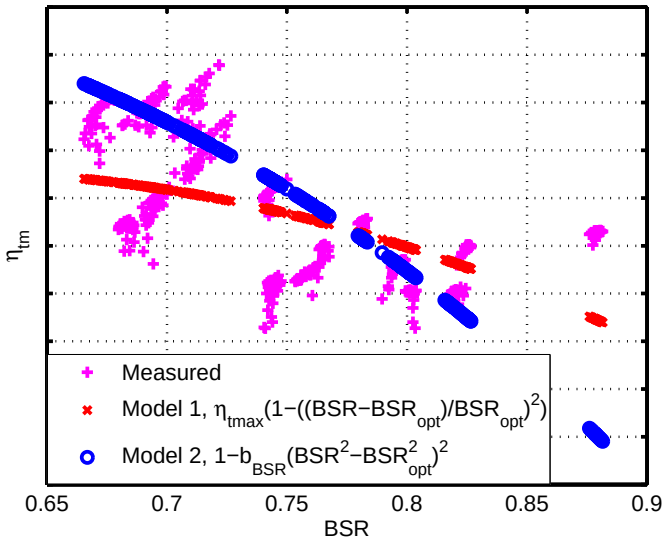

Figure 5.5. Two models for η_{tm} are plotted against measured η_{tm} caluculated through (5.11). Model 1, (5.9), gives a mean absolute relative error of 7.4 % and the corresponding value for model 2, i.e. the first factor in (5.14), is 9.4 %. Model 1 is used in the turbine model since the result is better for that one.

5.4 Implementation in Simulink

The model that has been developed in Sections 5.2 and 5.3 was implemented in the existing Simulink model, see [18]. The corrected mass flow through the turbine was modeled with (5.3). The mass flow through the wastegate was modeled with (5.1), where the effective area was given by (5.7). The turbine efficience was modeled with (5.9). In Figure 5.7, it can be seen that the flow through the turbine decreases when the wastegate opens. That leads to a decrease in turbine speed.

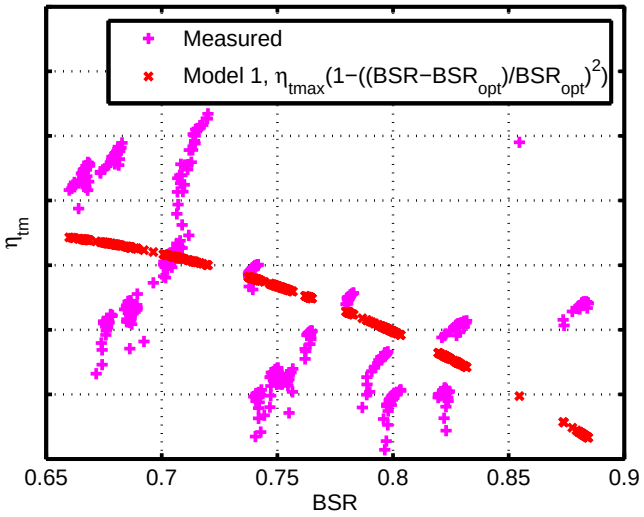

Figure 5.6. Model 1, (5.9), is validated against measured values for η_{tm} in data set 2. The mean absolute relative error is 7.4 %, which is the same as for the estimation data, data set 1.

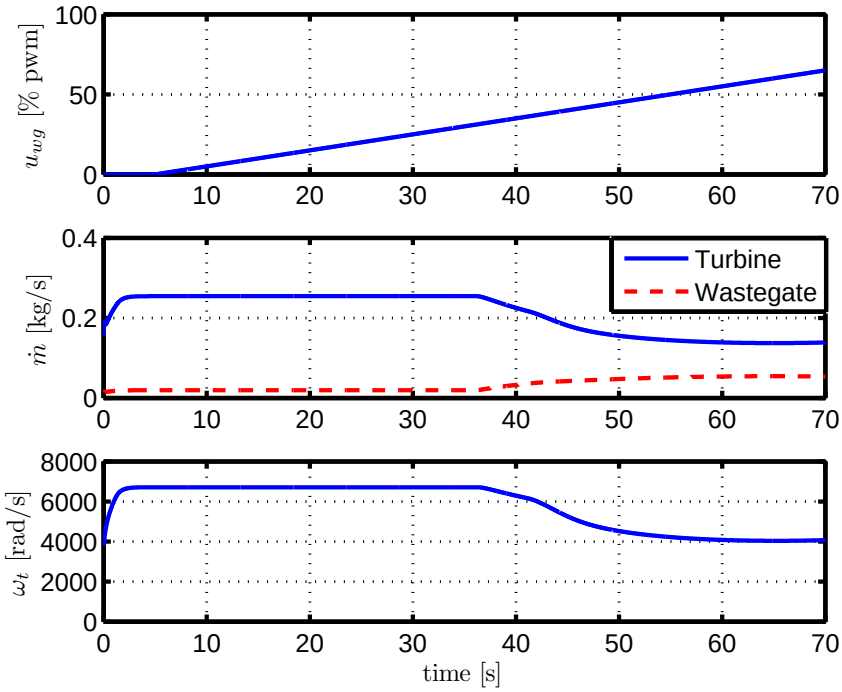

Figure 5.7. The performance of the implemented Simulink model for the wastegated turbine can be seen in this figure. In the upper plot, the wasegate goes from closed to open. The middle plot shows how the flow through the turbine decreases when the wastegate opens. That leads to a decrease in turbine speed, which can be seen in the lower plot.

Chapter 6

Control algorithm design

In this chapter, the control algorithm and the process of designing it is described. The primary objective is to control intake manifold pressure to meet requested engine torque with maintained oxygen-to-fuel ratio. The controller have been developed and tested with use of the CI engine model developed by J. Wahlström, which has been complemented with a wastegate sub-model.

Some nomenclature used in this chapter is first stated. The actuator position is denominated $\tilde{u}$, while requested position is plain u. When the signal is valid for both wastegate and VGT, the subscript $_t$ is used, i.e. u_t is turbine actuator requested position regardless of if the turbine is VGT or wastegated. Wastegate actuator signal is u_{wg} and VGT actuator signal is u_{vgt}.

6.1 Control objectives

The direct variable to be controlled is the turbocharger speed n_t, but the objective is to control intake manifold pressure p_{im} and air mass flow $\dot{m}_{ai}$. The goal is to follow a reference in p_{im} such that engine torque M_e could be produced fast enough while still maintaining low emissions. Suitable turbocharger speed is another goal, since high rotational speeds could damage the turbocharger. While a fast response to a requested intake manifold pressure is desired, an overshoot is undesired on the SI engine. The set point for λ_O for SI engines is close to 1, hence an overshoot in p_{im} could lead to an overshoot in M_e. The control objectives for the performance variables are the following.

1. A fast response to requested intake manifold pressure $p_{im,ref}$. Typical time constants for large steps are generally around 4 s.

2. Maximum 5 % overshoot in intake manifold pressure p_{im} for the SI engine

3. The turbocharger speed n_t is not allowed to exceed a maximum limit n_t^{max}

4. The controller should be easy to tune for different SI and CI engines

6.2 Control problems

In this section some specific problems encountered in the design of a turbocharger controller are described.

6.2.1 Control problems for VGT, sign reversal

The variable geometry turbine actuator can be described as a sliding wall with which the air inlet opening is changed. The change in opening affects both the flow resistance and how the inlet gas hit the vanes. The control problems encountered for the VGT are analysed through simulations on the diesel engine model developed by J. Wahlström. The channel from VGT input signal to turbine speed has a sign reversal, and the point where it occurs is here denoted u_{vgt}^{sgn}. As the VGT-actuator opens up, the gas flow resistance decreases and the flow for a given pressure ratio increases. Since mass flow is a factor in the turbine power, according to (4.14), increasing flow would lead to increasing turbine power. But at the same time, the inlet gas hit the turbine vanes at positions where the turbine efficiency decreases with increasing opening, leading to less turbine power and thus less turbine speed. The resulting turbine speed, as a function of VGT-signal in simulation on the engine model, is shown in Figure 6.1 when opening up the VGT. The input VGT-signal for all curves is a ramp from 0 % to 100 % at the same engine operating point: 2000 rpm and 100 mg fuel/cycle injected. The difference between the curves is the slope of the input VGT-signal ramp. As the figure shows, the maximum turbine speed is reached for different VGT-positions for the different curves, and the difference is as much as 20 percentage points. The ramp with slope 100 %/s has its maximum at 48 % VGT, and the ramp with slope 10 %/s has its maximum at just below 28 % VGT. If the VGT is instead closing, the result is somewhat different. In Figure 6.2, the result from closing the VGT with different ramps is shown. In this case, the result is that u_{vgt}^{sgn} does not differ much, but the maximum value in ω_t varies.

Since the turbocharger speed is output from a dynamic system, the behaviour is maybe not entirely surprising, but it makes the sign-reversal and maximum turbine power hard to calculate or predict. The sign reversal makes it hard to control the system, since an increasing VGT-signal at first increases the turbine speed but after the reversal it decreases it. Two different steps in VGT-signal are shown in Figure 6.4 where the step height in VGT is the same but with different starting values. The resulting turbine speed response is in the left plot an increase, and in the right plot a decrease. Furthermore, the rise time for the transient response from u_{vgt} to ω_t are quite different on each side of u_{vgt}^{sgn}, and the turbine efficiency η_{tm} is larger when $u_{vgt} > u_{vgt}^{sgn}$, as can be seen in Figure 6.3.

A linear controller implemented to control the system will give the behaviour seen for the first step in Figure 6.5, if the control signal is smaller than the sign-reversal point. If the controller is used for steps where the control signal exceeds the sign-reversal, the result is as shown in the last step in Figure 6.5. The explanation is that after the sign-reversal the turbocharger speed decreases with increasing control signal, whereby the controller increases the signal further, since the error

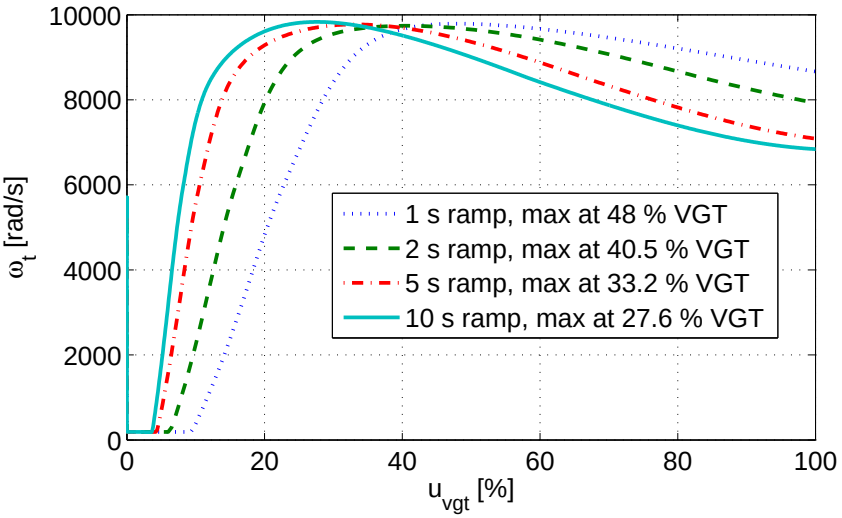

Figure 6.1. Simulated turbine speed responses when opening up the VGT with ramps with different slopes. The ramps all have starting value 0 % and final value 100 %, but the time differs from 1 s to 10 s, as described by the legend.

becomes larger. The result is a fast growing control signal.

6.2.2 Control problems for wastegated turbine

The wastegated turbine is controlled with a throttle. When the throttle opens, exhaust gases can bypass the fixed geometry turbine and the turbine speed decreases. The main problems is a long saturation. In Section 5.2.2 it is described that the pwm-signal is only effective in the range from 33 % to 65 %. Another thing is that the wastegate controller do not have the same flexibility as the VGT controller. In Figure 5.7 it is shown that the flow through the wastegate is only a small portion of the total flow.

The channel from wastegate input signal to turbine speed does not have a sign reversal, which makes the wastegated turbine easier to control than the VGT.

6.3 Choice of control approach

In order to be able to run the controller for different choices of turbines, with or without EGR, on SI or CI engines, an independent control approach for the turbine actuator is chosen. The main goal for the controller is to regulate p_{im}. Reference values in p_{im} and $\dot{m}_{ai}$ can be translated into a reference value in turbocharger speed, ω_t, via the compressor map. The turbocharger speed is controlled with a linear controller, with a state dependent non-linear compensator taking care of the non-linearities. A block-diagram showing the control structure is shown in

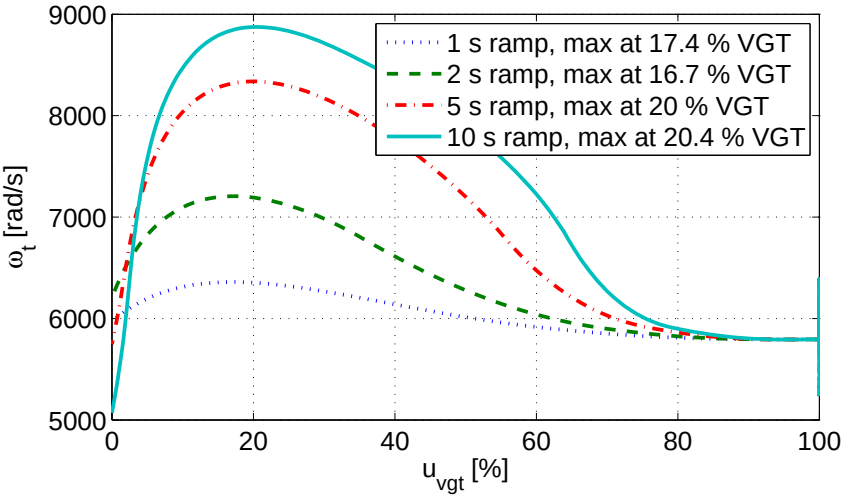

Figure 6.2. Simulated turbine speed responses when closing the VGT with ramps with different slopes. The ramps all have starting value 100 % and final value 0 %, but the time differs from 1 s to 10 s, as described by the legend.

Figure 6.6. With the non-linear block, the controller can be used to control the system M_{tm} to ω_t (represented by the block $G2$ in Figure 6.6), which is linear (see (6.1)). With an accurate static model inverse as non-linear block, the step response can be shaped in the linear system. The turbocharger speed is not measured, but estimated from intake manifold pressure and air mass flow using a compressor model. The same compressor model is used to create a reference in turbocharger speed from reference values in intake manifold pressure and air mass flow. To prevent integrator windup, tracking is used as anti-windup. The saturation limits is updated in the non-linaer block using the turbine model from turbine control signal to turbine torque.

6.3.1 Linear system

From M_{tm} to ω_t, the transfer function is of first order and linear

$$\frac{d\omega_t}{dt} = \frac{1}{J_t}\left(M_{tm} - M_c\right) \tag{6.1}$$

which could also be described by the block $G2$ in Figure 6.6:

$$G2 = \frac{1}{J_t s} \tag{6.2}$$

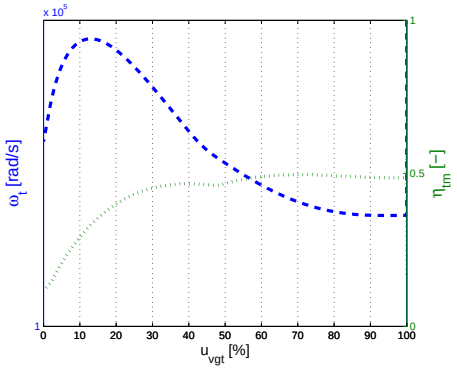

Figure 6.3. Turbocharger speed and turbine efficiency. The turbine efficiency is small to the left of u_{vgt}^{sgn}. The figure only shows one case in simulation and is intended to show only the small efficiency for small VGT-positions.

6.4 Reference signal generation

The control objective is to follow reference values in intake manifold pressure and air mass flow into the engine. These two variables are related through equation (6.3), where there is a linear relationship that is shown in Figure 6.7. The intake manifold pressure can be described by

$$p_{im} = \frac{\dot{m}_{ei} \cdot T_{im} \cdot 120 \cdot R_a}{\eta_{vol} \cdot n_e \cdot V_{cyl} \cdot n_{cyl}} \tag{6.3}$$

where η_{vol} is the volumetric efficiency, V_{cyl} is the cylinder displaced volume and n_{cyl} is the number of cylinders (see [18]). The intake manifold pressure is translated into reference value in compressor outlet pressure and the air mass flow into the engine is translated to reference value in air mass flow through the compressor. If no intake throttle is used, the pressure drop from compressor outlet to intake manifold could be modeled as an incompressible flow restriction with (6.4), and the air mass flows $\dot{m}_{ei}$ (minus EGR-mass flow) and $\dot{m}_c$ will be the same in stationary conditions.

$$\dot{m} = C_{ic}\sqrt{\frac{p_{ac}(p_{ac} - p_{im})}{R_a T_{ac}}} \Longrightarrow p_{ac} = \frac{p_{im}}{2} + \sqrt{\frac{p_{im}^2}{4} + \dot{m}^2 T_{ac}\frac{R_a}{C_{ic}^2}} \tag{6.4}$$

The reference signal in turbocharger speed is derived from reference values in intake manifold pressure and air mass flow. In Figure 6.8 a typical compressor map is shown, and the derivation of rotational speed from pressure ratio over the compressor and air mass flow through it is obvious. Rotational speed is derived from extrapolated compressor maps provided by Scania CV. The pressure ratio Π_c is the ratio between pressure after and before the compressor and is defined as

$$\Pi_c = \frac{p_{ac}}{p_{bc}} \tag{6.5}$$

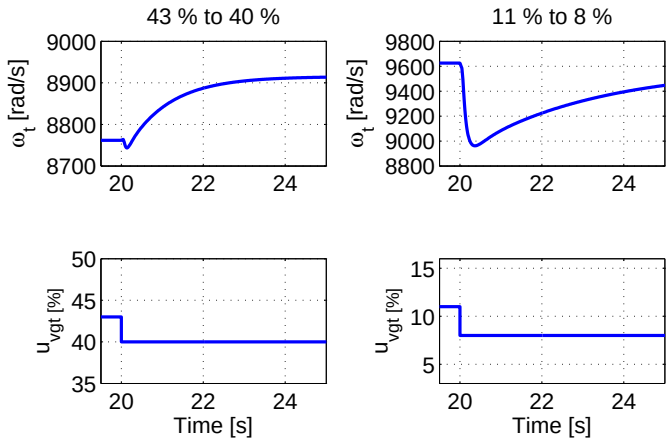

Figure 6.4. Steps in VGT-signal showing resulting turbocharger speed. The left plot shows a step from 43 % to 40 % VGT, and the right plot shows a step with the same amplitude but from 11 % to 8 % VGT. The resulting turbocharger speeds are very different, since the system is non-linear and there is a sign reversal.

where the pressure before the compressor p_{bc} is derived from the ambient pressure p_{amb} in (6.6), which uses the same equation for incompressible flow restriction as used in (6.4).

$$\dot{m} = C_{airf}\sqrt{\frac{p_{amb}(p_{amb}-p_{bc})}{R_a T_{amb}}} \Longrightarrow p_{bc} = p_{amb} - \frac{\dot{m}^2 R_a T_{amb}}{C_{airf}^2 p_{amb}} \tag{6.6}$$

The parameters C_{ic} and C_{airf} are modeled as constant for the specific intercooler and airfilter.

6.5 Compensating for non-linearities

In this section, the non-linear compensator (the block "Non-linear block, Static inverse" in Figure 6.6) is described. The main idea is to transform a turbine torque input signal to an input signal in turbine actuator position. This is performed by running the signal through a static inverse of a turbine model.

6.5.1 Feedback loop

The chosen feedback loop is ω_t estimated from measured p_{im}. By filtering p_{im} and $\dot{m}_{ai}$ (estimated with volumetric efficiency) through the same filter that the reference signal is generated with (i.e. Equations (6.4), (6.6) and the compressor map), the controller receives a single input, ω_t. It should be noted that, in order to avoid the problem with the sign-reversal, the choice of another feedback-loop would make sense. In [19], the chosen feedback for turbocharger control is p_{em},

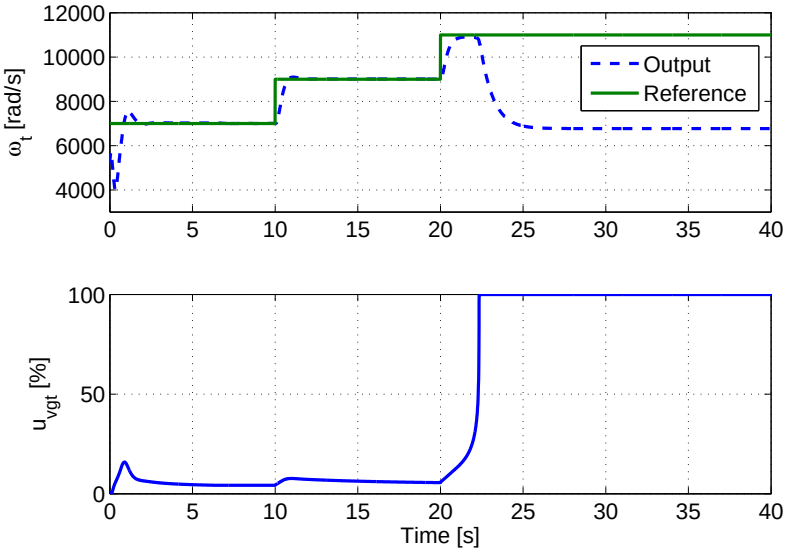

Figure 6.5. Step responses to increasing turbocharger speeds. For the step from 7000 rad/s to 9000 rad/s, the controller puts out signals below u_{vgt}^{sgn}, but in the step from 9000 rad/s to 11000 rad/s the output signal exceeds this point with a resulting drop in turbocharger speed. The control signal is quickly increasing to its maximum value when the signal exceeds u_{vgt}^{sgn} as the control error increases.

but with the control objectives in this work in mind, p_{im} is chosen and the problem with the sign-reversal remains.

6.5.2 Non-linear compensator

The non-linear compensator is constructed through inverting the model for turbine power, with actuator position $\tilde{u}_t$ as input and turbine power including mechanical power losses, P_{tm}, as output. A non-linear compensator for the VGT is first presented, followed by the wastegate turbine.

VGT

A model from VGT actuator position, $\tilde{u}_{vgt}$, to turbine power including mechanical power losses, P_{tm}, is presented in [18], and is also used in this paper. The model

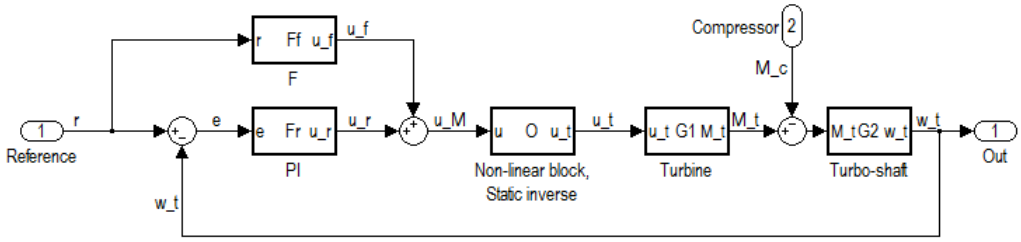

Figure 6.6. The figure shows the chosen control structure, with reference value in ω_t and a non-linear block. The figure excludes the actual feedback loop which has p_{im} as output. This is further explained in Section 6.4.

follows from equations (6.7) to (6.16).

$$P_{tm} = P_{t,ideal} \cdot \underbrace{\eta_t \cdot \eta_m}_{\eta_{tm}} = \dot{m}_t c_{pe} T_{em} \left(1 - \Pi_t^{1-\frac{1}{\gamma_e}}\right) \eta_{tm} \tag{6.7}$$

$$\dot{m}_t = \frac{A_{vgt,max} p_{em} f_\Pi(\Pi_t) f_\omega(\omega_t) f_{vgt}(\tilde{u}_{vgt})}{\sqrt{T_{em} R_e}} \tag{6.8}$$

$$f_\Pi(\Pi_t) = \sqrt{1 - \Pi_t^{\kappa_t}} \tag{6.9}$$

$$f_\omega(\omega_t) = 1 - c_{\omega t}\left(\frac{\omega_t}{100\sqrt{T_{em}}} - \omega_{t,corropt}\right)^2 \tag{6.10}$$

$$f_{vgt}(\tilde{u}_{vgt}) = c_{f2} + c_{f1}\sqrt{max\{0, 1 - \left(\frac{\tilde{u}_{vgt} - c_{vgt2}}{c_{vgt1}}\right)^2\}} \tag{6.11}$$

$$\eta_{tm} = \eta_{tm,BSR}(BSR) \cdot \eta_{tm,\omega}(\omega_t) \cdot \eta_{tm,vgt}(\tilde{u}_{vgt}) \tag{6.12}$$

$$\eta_{tm,BSR}(BSR) = 1 - b_{BSR}\left(BSR^2 - BSR_{opt}^2\right)^2 \tag{6.13}$$

$$BSR = \frac{R_t \omega_t}{\sqrt{2 c_{pe} T_{em}\left(1 - \Pi_t^{1-1/\gamma_e}\right)}} \tag{6.14}$$

$$\eta_{tm,\omega}(\omega_t) = \begin{cases} 1 - b_{\omega t1}\omega_t & \text{if } \omega_t \le \omega_{t,lim}, \\ 1 - b_{\omega t1}\omega_{t,lim} - b_{\omega t2}(\omega_t - \omega_{t,lim}) & \text{if } \omega_t > \omega_{t,lim} \end{cases} \tag{6.15}$$

$$\eta_{tm,vgt}(\tilde{u}_{vgt}) = b_{vgt1}\tilde{u}_{vgt}^3 + b_{vgt2}\tilde{u}_{vgt}^2 + b_{vgt3}\tilde{u}_{vgt} + b_{vgt4} \tag{6.16}$$

The inverted model from M_{tm} to $\tilde{u}_{vgt}$ is derived through inverting (6.11), and

$$M_{tm} = \frac{P_{tm}}{\omega_t} \tag{6.17}$$

and all other equations are treated as state dependent coefficients. The turbine efficiency, η_{tm} in (6.12), is also treated as a state dependent coefficient, with $\tilde{u}_{vgt}$ as measured input. The inverted model thus becomes as depicted in equations (6.18) to (6.21).

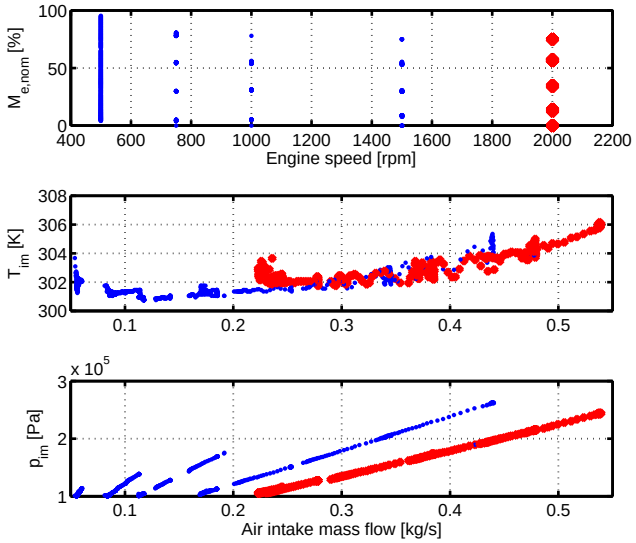

Figure 6.7. This figure shows the linear relationship between intake manifold pressure p_{im} and air intake mass flow $\dot{m}_{ai}$, where the slope mainly change with engine speed. The red and bold markers in the figure show all data points collected at engine speed 2000 rpm. The linear relationship is described by (6.3).

$$u_{vgt}(t) = \tilde{u}_{vgt}(t) \tag{6.18}$$

$$\tilde{u}_{vgt} = c_{vgt2} - c_{vgt1}\sqrt{max\{0, 1 - \Big(\frac{max\{0, f_{vgt} - c_{f2}\}}{c_{f1}}\Big)^2\}} \tag{6.19}$$

$$f_{vgt} = \frac{\dot{m}_t\sqrt{R_e T_{em}}}{A_{vgt,max} p_{em} f_\Pi f_\omega} \tag{6.20}$$

$$\dot{m}_t = \frac{P_{tm}}{c_{pe} T_{em}\Big(1 - \Pi_t^{1-1/\gamma_e}\Big)\eta_{tm}} \tag{6.21}$$

In (6.18), the VGT actuator is assumed to be ideal, and (6.19) is valid within the saturation limits $\tilde{u}_{vgt}^{max}$ and $\tilde{u}_{vgt}^{min}$. Equation (6.19) is derived from (6.11), (6.20) is derived from from (6.8) and (6.21) from (6.7).

The equations above describe the controller output when $\tilde{u}_{vgt} < \tilde{u}_{vgt}^{sgn}$. If the controller is to work for outputs from $\tilde{u}_{vgt}^{sgn}$ to 100 % (open), (6.18) has to be changed to

$$u_{vgt}(t) = 100 - \tilde{u}_{vgt}(t) \tag{6.22}$$

Under operating conditions where intake manifold pressure build-up is the primary controller objective, it is desirable to have as open VGT as possible in order to

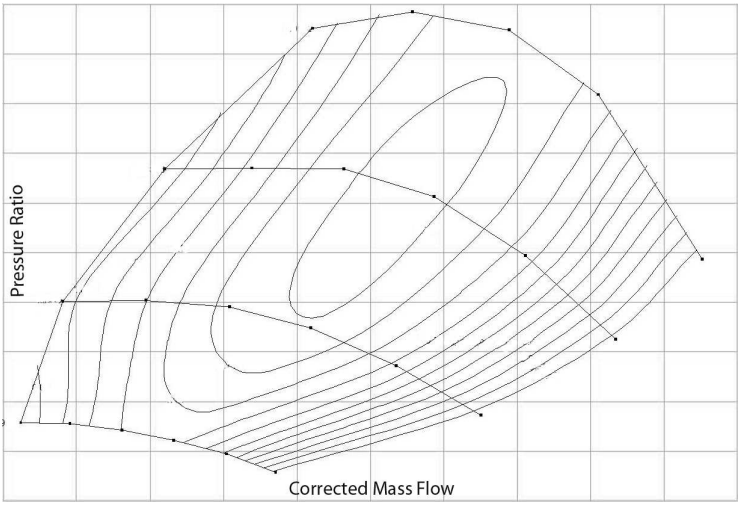

Figure 6.8. A typical compressor map with the corrected mass flow on the x-axis and the pressure ratio on the y-axis. The horizontal lines are constant speed lines and the "islands" show constant efficiency.

minimize pumping losses. But there are situations where the VGT have to close, for example to build up exhaust pressure in gear changes and to drive EGR. The problem is to find exactly where the sign-reversal occurs, which has been proven to be very difficult.

Wastegated turbine

A model from wastegate pwm-signal to turbine power is presented in Section 5 with equations (5.1), (5.7) and (5.13). The inverted model becomes (6.23) to (6.26).

$$u_{wg} = \frac{-d_{A2}}{2d_{A1}} - \sqrt{\left(\frac{d_{A2}}{2d_{A1}}\right)^2 - \frac{d_{A3} - A_{wg}}{d_{A1}}} \tag{6.23}$$

$$A_{wg} = \frac{\dot{m}_t \sqrt{R_e T_{em}}}{p_{em} \Psi\left(\Pi_t\right)} \tag{6.24}$$

$$\dot{m}_t = \frac{P_{tm}}{\eta_{tm} c_{pe} T_{em} \left(1 - \Pi_t^{(1-1/\gamma_e)}\right)} \tag{6.25}$$

$$M_{tm} = \frac{P_{tm}}{\omega_t} \tag{6.26}$$

where $\Psi\left(\Pi_t\right)$ is defined in (5.2) and η_{tm} is approximated with a constant. It would have been more precise to model η_{tm} as suggested in (5.9) but as seen in Figure 5.6 the values does not vary much in the region where test data exist. Therefore it can be described by a constant, without losing significant accuracy.

6.6 Linear controller

The linear controller is designed to control the system (6.2), and a proportional and integral controller with feedforward (PIFF) is chosen. The controller parameters are chosen through pole placement, where the time constant for the closed loop system is chosen to give a desired rise time for the system. The objective is a fast response to requested p_{im} with no overshoot for the SI engine. By the approach with a simple linear controller in combination with a non-linear compensator, the tuning of controller parameters becomes easy. The linear controller is given by

$$u'(t) = K_F \cdot \omega_{ref}(t) + K_P \cdot e(t) + \int_0^t \left(e(\tau) + \frac{1}{K_P} \left(\bar{u}'(\tau) - u'(\tau) \right) \right) d\tau \tag{6.27}$$

$$e(t) = \omega_{ref}(t) - \omega(t) \tag{6.28}$$

where the parameters K_F, K_P and K_I are static gains. The term $\frac{1}{K_P}\left(\bar{u}'(\tau) - u'(\tau)\right)$ is added to the integral part of the control signal in order to avoid integrator wind-up. The method is called back-stepping and is further described in Section 6.6.1.

A step response for the system (6.2) controlled by the linear controller (6.27) - (6.28) is shown in Figure 6.9, where the gains K_F, K_P and K_I are chosen to give the closed loop system (6.32) the time constant 4 s. The gains are chosen by pole placement of the closed loop system.

$$G_c = \frac{G\left(F_f + F_r\right)}{1 + GF_r} \tag{6.29}$$

$$F_f = K_F \tag{6.30}$$

$$F_R = K_P + \frac{K_I}{s} \tag{6.31}$$

$$G_c = \frac{s\left(K_F + K_P\right) + K_I}{\tau_{sys} s^2 + K_P s + K_I} \tag{6.32}$$

$$\tau_{sys} = J_t \tag{6.33}$$

From (6.32), the pole polynomial

$$p = J_t s^2 + K_P s + K_I = J_t \left(\left(s + \frac{K_P}{2J_t} \right)^2 - \frac{1}{J_t} \left(K_I - \frac{K_P^2}{4J_t} \right) \right) \tag{6.34}$$

is given, and in order to give the closed loop system the desired time constant τ_c, the poles are to be placed with distance

$$a = \frac{1}{\tau_c} \tag{6.35}$$

from the origin ([4]). In order to get a well damped system, the poles are placed on the real axis, i.e. in $(-a, 0)$, which gives the desired pole polynomial

$$p_{des} = (s + a)^2 \Rightarrow \begin{cases} \frac{K_P}{2J_t} & = a \\ \frac{1}{J_t}\left(K_I - \frac{K_P^2}{4J_t} \right) & = 0 \end{cases} \tag{6.36}$$

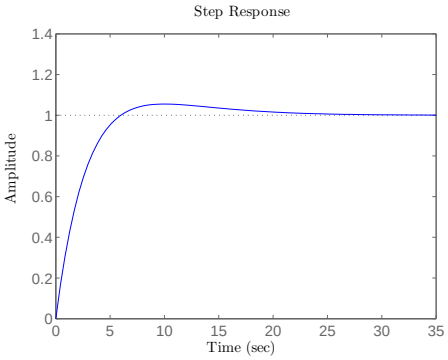

Figure 6.9. Step response for system system (6.2) controlled by the linear controller (6.27)

leading to feedback gains

$$K_P = 2J_t a = \frac{2J_t}{\tau_c} \tag{6.37}$$

$$K_I = J_t a^2 = \frac{J_t}{\tau_c^2} \tag{6.38}$$

In order to keep the closed loop system non-minimum phase, the feed forward gain K_F has to be chosen such that the zero polynomial, z, for the system (6.32) fulfils

$$z = s\left(K_F + K_P\right) + K_I = 0 \text{ for } \Re(s) < 0 \tag{6.39}$$

i.e. with no zeros in the right hand complex plane.

6.6.1 Integrator wind-up

When using integral control on systems where the control signal is saturated, the problem of integrator wind-up occurs. If not compensated for, the integral part will continue to integrate the error even when the control signal is saturated, leading to a growing controller output. When the control error finally decreases, it will take longer than necessary for the controller output to decrease.

To avoid this problem, there is a simple method called back-stepping (see [5]). The following reasoning is the basis for the algorithm: If the control error $e(t)$ would have been smaller, the saturation limit for $u(t)$ would not have been reached. There is a value for the control error that precisely saturates the controller output, i.e. gives the controller output the saturated value $\bar{u}(t)$. Call that value of the control error $\bar{e}(t)$. Applied to a PI-controller, this becomes

$$\bar{u}(t) = K_P \cdot \bar{e}(t) + K_I \cdot I(t) \tag{6.40}$$

where $I(t)$ is the integrated error. Subtracting the regular PI-controller from (6.40)

$$\bar{u}(t) - u(t) = K_P\left(\bar{e}(t) - e(t)\right) \Rightarrow \bar{e}(t) = e(t) + \frac{1}{K_P}\left(\bar{u}(t) - u(t)\right) \tag{6.41}$$

the error $\bar{e}(t)$ can be calculated. Using this in a new PI-controller

$$u(t) = K_P \cdot e(t) + K_I \cdot I(t) \tag{6.42}$$

$$\bar{u}(t) = sat\,(u(t)) \tag{6.43}$$

$$I(t) = \int_0^t e(\tau) + \frac{1}{K_P}\,(\bar{u}(\tau) - u(\tau))\,d\tau \tag{6.44}$$

the integrator wind-up is avoided. See Figure 6.10 for a Simulink-implementation of the algorithm. The saturation limits in $u'(t)$ are described in Section 6.7.

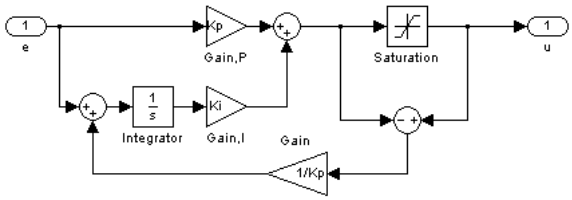

Figure 6.10. Block diagram showing tracking for a PI-controller. Tracking is used to avoid integrator wind-up.

6.7 Saturation levels

6.7.1 VGT

The saturation limits in u'^{min} and u'^{max} are produced by transforming the saturation limits u_{vgt}^{min} and u_{vgt}^{max} with the static turbine model (6.7) - (6.16). The turbine power P_{tm} is then divided with ω_t to get limits in turbine torque M_{tm}.

$$u'^{min/max} = \frac{P_{tm}(\tilde{u}_{vgt}^{min/max})}{\omega_{t,ref}} \tag{6.45}$$

$$= \frac{A_{vgt,max} p_{em} f_\Pi(\Pi_t) f_\omega(\omega_t) f_{vgt}(\tilde{u}_{vgt}^{min/max})}{\sqrt{T_{em} R_e}\,\omega_{t,ref}} c_{pe} T_{em} \left(1 - \Pi_t^{1-\frac{1}{\gamma_e}}\right) \eta_{tm} \tag{6.46}$$

6.7.2 Wastegated turbine

The saturation limits for the wastegated turbine is calculated using (5.13) with

$$\dot{m}_t = \dot{m}_{eo} - \dot{m}_{wg} \tag{6.47}$$

where $\dot{m}_{eo}$ is estimated from measures and $\dot{m}_{wg}$ is estimated from (5.1) with $A_{eff} = A_{wg}$ in (5.6). Furthermore, η_{tm} is inserted as the only factor for turbine efficiency in P_{tm}. The saturation limits is then given by (6.45). The pwm-signal is only effective in the range from 33 % to 65 % but since the area is only strictly increasing to 60 %, see Figure 5.3, that becomes the upper limit.

6.8 The complete controller

The complete controller, from reference value and feedback in turbocharger angular velocity ω_t to control signal to the turbine actuator u is presented here.

The *linear controller* produces a control signal $u'(t)$ to the non-linear compensator:

$$u'(t) = K_F \cdot \omega_{ref}(t) + K_P \cdot e(t) + K_I \int_0^t \left(e(\tau) + \frac{1}{K_P} \left(\bar{u}(\tau) - u(\tau) \right) \right) d\tau \quad (6.48)$$

$$e(t) = \omega_{ref}(t) - \omega(t) \quad (6.49)$$

The *non-linear compensator* produces a control signal $u(t)$ to the turbine actuator:

$$u(t, t-1) = \tilde{u}(t, t-1) \text{ (ideal actuator)} \quad (6.50)$$

$$\tilde{u}(t, t-1) = c_{vgt2} - c_{vgt1} \sqrt{max\{0, 1 - \left(\frac{max\{0, f_{vgt}(t, t-1) - c_{f2}\}}{c_{f1}} \right)^2\}} \quad (6.51)$$

$$f_{vgt}(t, t-1) = \frac{\dot{m}_t(t, t-1)\sqrt{R_e T_{em}}}{A_{vgt,max} p_{em} f_\Pi f_\omega} \quad (6.52)$$

$$\dot{m}_t(t, t-1) = \frac{u'(t) \cdot \omega_{ref}(t)}{c_{pe} T_{em} \left(1 - \Pi_t^{1-1/\gamma_e} \right) \eta_{tm}(\tilde{u}(t-1))} \quad (6.53)$$

$$\eta_{tm}(\tilde{u}(t-1)) = \eta_{tm,\omega_t} \cdot \eta_{tm,BSR} \cdot \eta_{tm,vgt}(\tilde{u}(t-1)) \quad (6.54)$$

$$\eta_{tm,vgt}(\tilde{u}(t-1)) = b_{vgt1}\tilde{u}^3(t-1) + b_{vgt2}\tilde{u}^2(t-1) + b_{vgt3}\tilde{u}(t-1) + b_{vgt4} \quad (6.55)$$

Note that η_{tm} depend on the actuator position $\tilde{u}_{vgt}$ through feeding back the actuator position, thereby the dependency on $(t-1)$.

The wastegate actuator control signal is produced by transforming $u'(t)$ with Equations (6.23) to (6.26).

6.9 Results

The results from simulations with the controller are presented here. First, results from simulations with VGT is given, followed by results from simulations with wastegate.

6.9.1 VGT

The results from simulations are that the linear controller is easy to tune for shaping of the step response. A step in ω_t is shown in Figure 6.13. To test the controller on more realistic reference signals, signals collected during field tests were used as reference to see how the controller manage to follow those signals. The signals were collected with sample frequency 10 Hz, and are low-pass filtered to get rid of some measurement noise.

First, the controller is tested with ω_t as feedback and reference. The input turbocharger speed is saturated at 5300 rad/s, since $u_{vgt} > u_{vgt}^{sgn}$ cannot produce speeds below this at some of the investigated engine operating regions. Furthermore, the primary control objective is to produce a fast boost pressure build-up in order to give a fast torque response with desired λ. Worth to mention is that the signal used as reference is a field test output signal and not a reference. If the controller (6.18) is used, i.e. when $u_{vgt} < u_{vgt}^{sgn}$, the result is as shown in Figure 6.11. If the controller (6.22) is used, i.e. when $u_{vgt} > u_{vgt}^{sgn}$, the result is a somewhat slower response. This is could be intuitively explained by looking at Figure 6.1, where it can be seen that a linearized system with transfer function from u_{vgt} to ω_t would have a larger time constant for $u_{vgt} > u_{vgt}^{sgn}$. The result when following the reference in ω_t is shown in Figure 6.12.

When controlling p_{im}, the results are similar to the ones when controlling ω_t. Step responses in p_{im} are shown in Figures 6.14 and 6.15. In the two figures, $u_{vgt} < u_{vgt}^{sgn}$ in one and $u_{vgt} > u_{vgt}^{sgn}$ in the other, which causes quite large differences between the rise times. Furthermore, p_{im} cannot reach the same pressures in the two cases, as illustrated by Figures 6.21 and 6.22. It can also be noted that the different engine speeds in the two figures pose different maximum and minimum limits for p_{im} since $\dot{m}_{eo}$ increase with increasing engine speed and torque. This makes the testing with 'real' signals a bit tricky, since the field tests are run with fast changing engine speed and torque. An interval where there were reachable levels in p_{im} was thus chosen as reference.

The results from simulations with a field test signal as reference is shown in Figures 6.18 and 6.17. Once again, the controller with $u_{vgt} < u_{vgt}^{sgn}$ is faster.

The control objective $n_t < n_t^{max}$ would be easy to satisfy if n_t was measured, by simply introducing an upper limit for the requested turbocharger speed. VGT:s generally have sensors for measuring n_t, but wastegated turbines most commonly have not. Thereby the speed control rely on the compressor map based model with which reference and feedback values are generated. It is assumed that the model is accurate, which would make the speed limit straightforward to implement.

6.9.2 Wastegate

In Figure 6.23, it can be seen that the wasegate controller have a time constant below 4 s with small overshoots. It is also easy to tune the controller to get this performance. Compared to the VGT controller it is easier to get desired behaviour of the system, considering that there is no sign reversel for the control signal. The range for reachable turbine speed is 6100 rad/s to 8400 rad/s for engine speed of 2000 rpm and 120 mg fuel/cycle injected.

6.9.3 Robustness

To test the robustness of the controller, errors were introduced to the parameters in the non-linear compensator and the controller was tested with these errors. These tests show that small modeling errors in the parameters in $\eta_{tm,BSR}$ introduced oscillations in the system if the error is positive. When looking at the $\eta_{tm,BSR}$

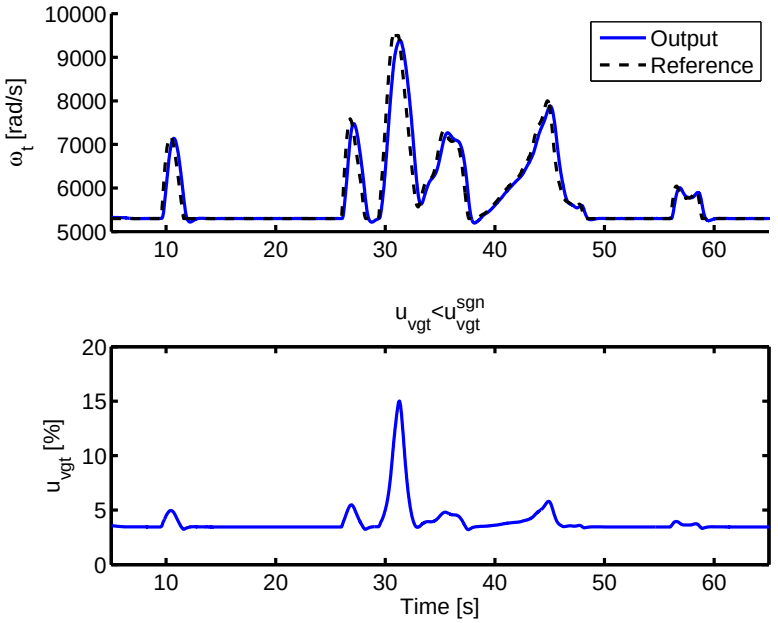

Figure 6.11. The figure shows how the controller manages to follow a reference in ω_t and the produced controller output, when $u_{vgt} < u_{vgt}^{sgn}$. The signal used as reference is collected from field tests, but note that the signal is a measured output signal and not a reference signal during the test. Engine speed is 1500 rpm and 120 mg fuel/cycle is injected.

model, it is seen that values of BSR_{opt} just above the original parameter value gives $\eta_{tm,BSR} = 0$ for low BSR, which means the controller output is gained to infinity (see (6.21)). Therefore, when choosing the parameter BSR_{opt}, it is of great importance to choose a value that do not give $\eta_{tm,BSR} = 0$. Even negative modeling errors in BSR_{opt} affected the performance, since they make the modeled turbine efficiency too large and hence gain the controller output with gain less than one. According to Figure 6.24, even small errors in BSR_{opt} give large variations in $\eta_{tm,BSR}$, especially for small BSR. The other parameter in $\eta_{tm,BSR}$, b_{BSR} is not as sensitive as BSR_{opt} but is definitely influencing the control signal gain. Next to $\eta_{tm,BSR}$ in sensitivity is the sub-model for flow depending on $\tilde{u}_{vgt}$ in (6.11). The parameter b_{vgt2} is changing the control signal gain already at modeling errors of 10 %, and at errors of more than 20 % the gain becomes far too large for the controller to work properly. The parameters b_{vgt1} and b_{vgt3} manage errors of up to about 20 % but larger errors introduce oscillations. The parameter b_{vgt4} is rather insensitive to modeling errors, since it gains the signal equally much over the entire $\tilde{u}_{vgt}$ domain. It should be noted that the value of b_{vgt3} when optimized for the CI engine model is very small, that is why changes in does not affect more

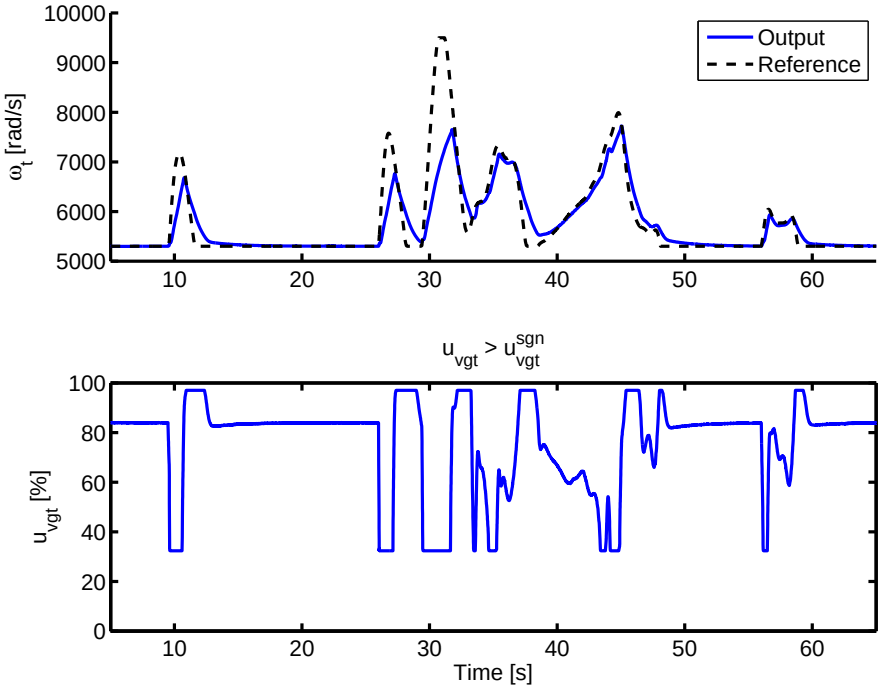

Figure 6.12. The figure shows how the controller manages to follow a reference in ω_t and the produced controller output, when $u_{vgt} > u_{vgt}^{sgn}$. The signal used as reference is collected from field tests, but note that the signal is a measured output signal and not a reference signal during the test. Engine speed is 1500 rpm and 120 mg fuel/cycle is injected.

than it does.

The other parameters are more tolerant against modeling errors. When changing the parameters one at a time, the change in controller performance is hardly noticeable for parameter modeling errors of ±10 %. For modeling errors of about 20 %, the parameters c_{vgt1} and c_{vgt2} in sub-model (6.11) start to affect performance by gaining the signal too much or too little. For modeling errors of about 50 %, c_{vgt1} and c_{vgt2} change the controller output completely, and the parameter c_{f1}, introduce oscillations. The parameter $A_{vgt,max}$ is a pure gain of the signal, changing it gains it independently of the engine states.

6.9.4 Simplifications

One objective is for the controller to be easy to tune. Thereby some further simplifications are desired, and the performance is evaluated with these simplifications.

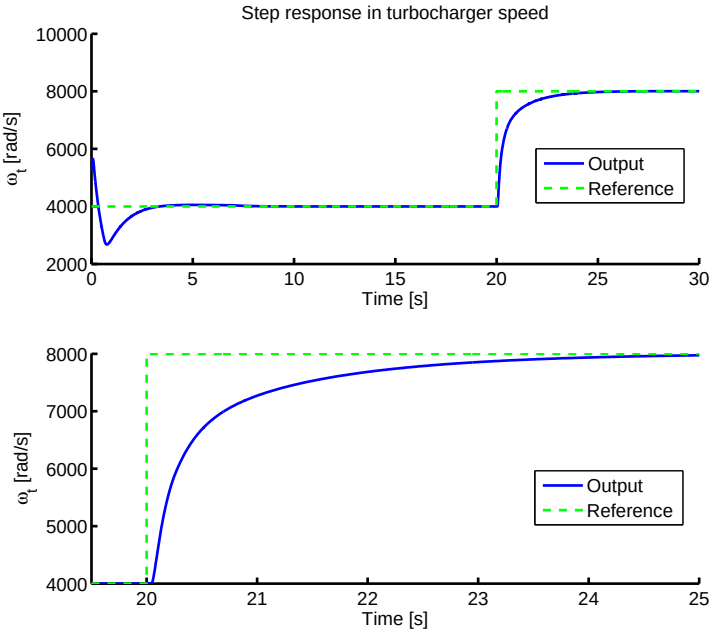

Figure 6.13. A step in requested ω_t and the response produced by the controller. Engine speed is 1500 rpm and 120 mg fuel/cycle is injected.

During the robustness testing, it was revealed that some parameters had low influence on the DC-gain, and were therefore removed from the inverted model in the controller.

One parameter that has very little influence is $b_{\omega t2}$ in the $\eta_{tm,\omega}$ sub-model. In Figure 6.25, $\eta_{tm,\omega}$ is plotted as a function of ω_t, and as seen removal of the parameter $b_{\omega t2}$ does not change the curve much. Another factor that is very insensitive to modeling errors is f_ω in the sub-model for turbine flow (6.10). Changing the parameters $c_{\omega t}$ and $\omega_{t,corropt}$ 50 % does not change the controller performance to any extent.

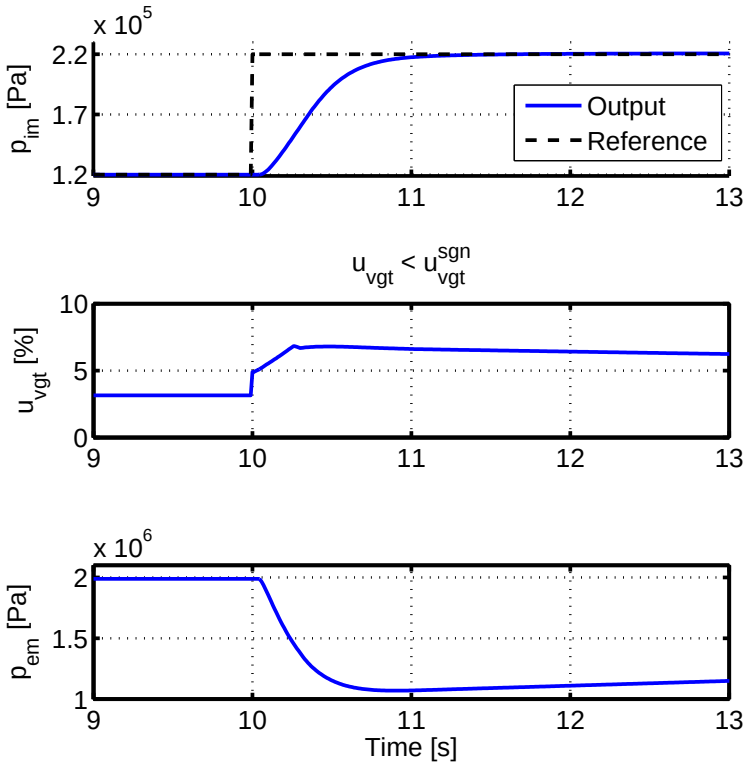

Figure 6.14. Step response for step in requested p_{im}, when $u_{vgt} < u_{vgt}^{sgn}$. The resulting step response is very fast and the overshoot is only 0.3 %, but p_{em} is large. Engine operating point: 1500 rpm and 120 mg/cycle.

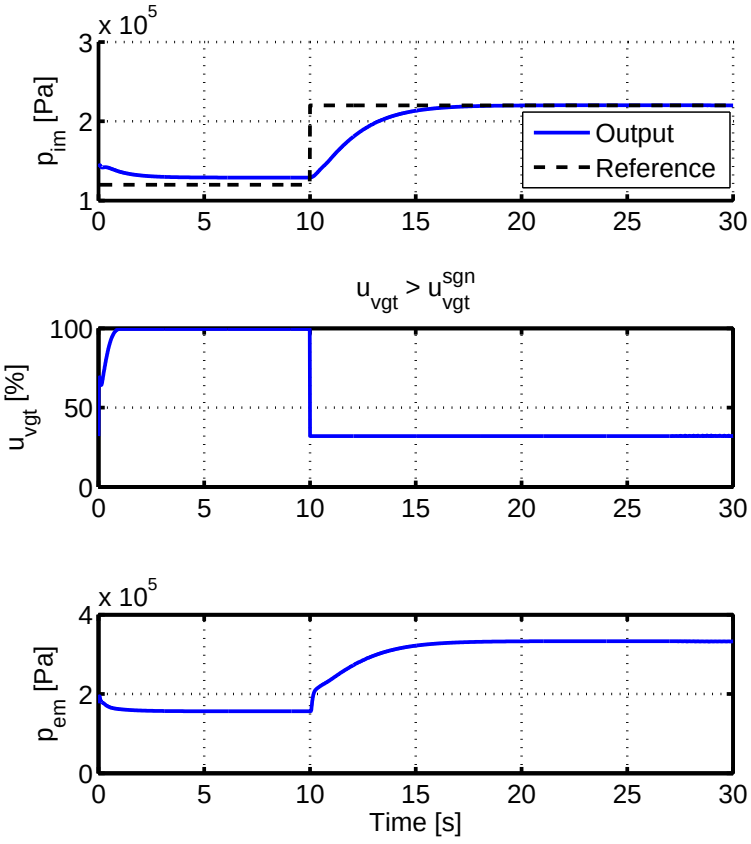

Figure 6.15. Step response for step in requested p_{im}, when $u_{vgt} > u_{vgt}^{sgn}$. The resulting step response is slower without overshoot, and p_{em} is about 10 times smaller for the step in Figure 6.14. The control signal is saturated in almost the entire simulation time, and the starting value of the reference value cannot be reached. Due to the anti wind-up algorithm the step response is still fast. Engine operating point: 1500 rpm and 120 mg/cycle.

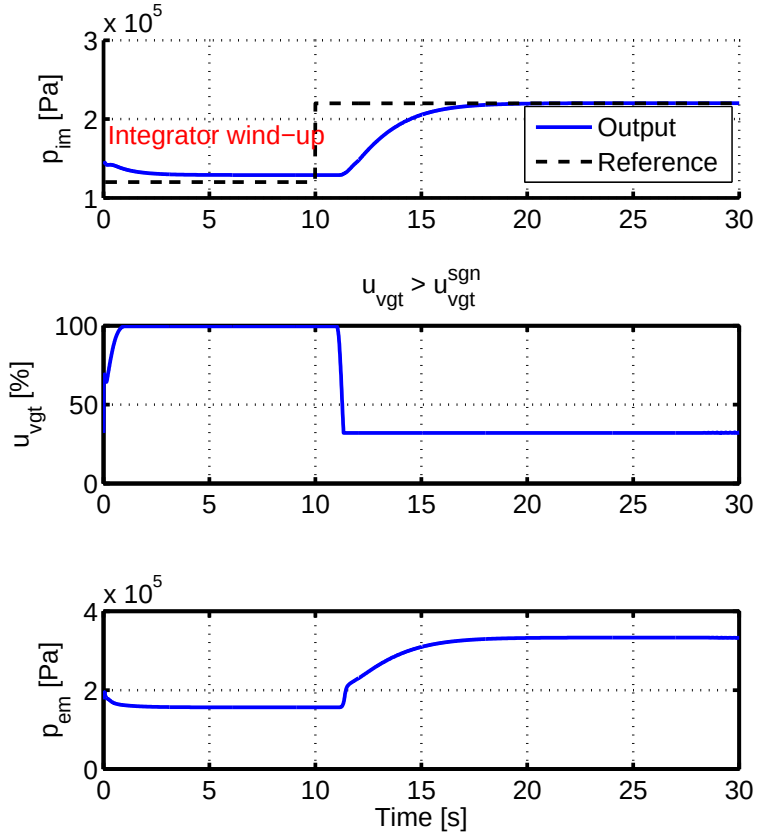

Figure 6.16. The same step as in Figure 6.15, but without anti wind-up. The result is a time lag in the response. Engine operating point: 1500 rpm and 120 mg/cycle.

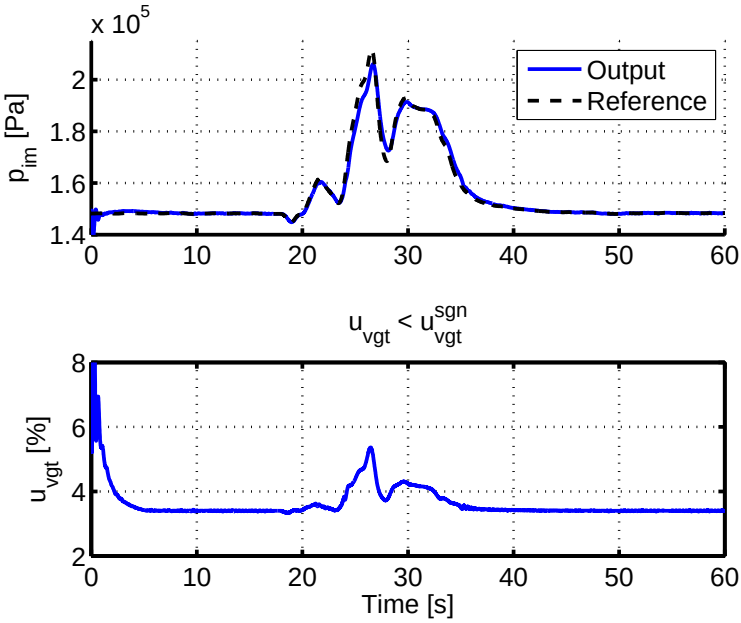

Figure 6.17. The figure shows how the controller manages to follow a reference in p_{im} and the produced controller output, when $u_{vgt} < u_{vgt}^{sgn}$. The signal used as reference is collected from field tests, but note that the signal is a measured output signal and not a reference signal during the test. Engine speed is 1500 rpm and 120 mg fuel/cycle is injected.

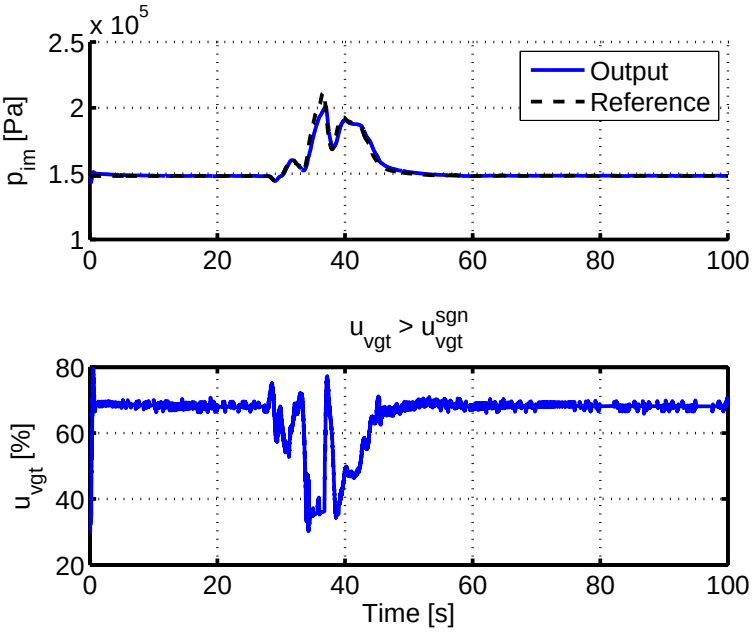

Figure 6.18. The figure shows how the controller manages to follow the same reference in p_{im} as in Figure 6.17 and the produced controller output, when $u_{vgt} > u_{vgt}^{sgn}$. The signal used as reference is collected from field tests, but note that the signal is a measured output signal and not a reference signal during the test. Engine speed is 1500 rpm and 120 mg fuel/cycle is injected.

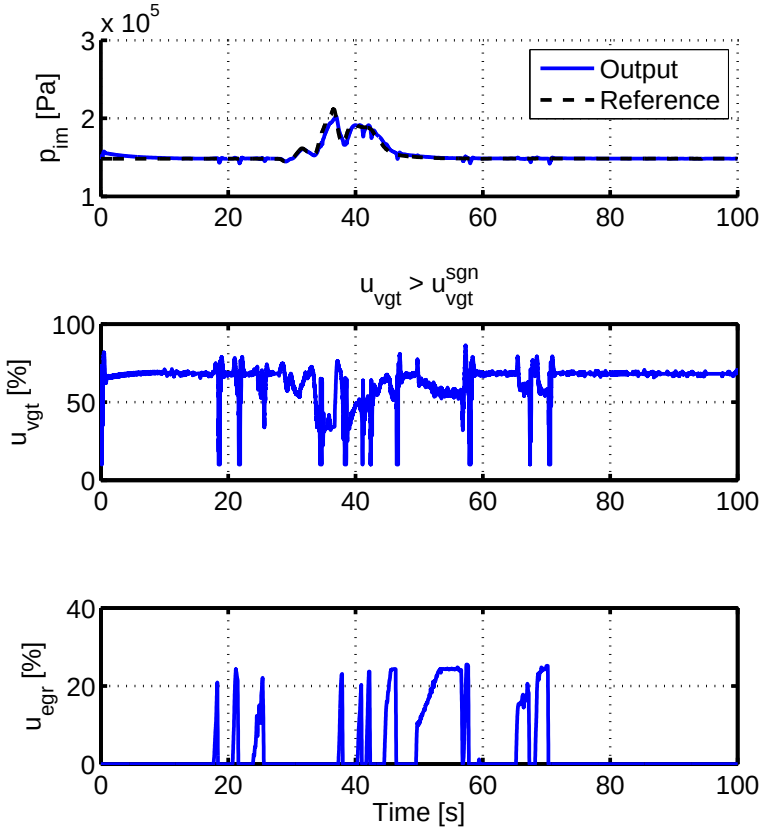

Figure 6.19. The figure shows how the controller manages to follow the same reference in p_{im} as in Figure 6.17 and the produced controller output, when $u_{vgt} > u_{vgt}^{sgn}$ and when the EGR-signal to the system is quite aggressive. The controller still manages to follow the reference. The signal used as reference and the EGR input signal is collected from field tests, but note that the signal is a measured output signal and not a reference signal during the test. Engine speed is 1500 rpm and 120 mg fuel/cycle is injected.

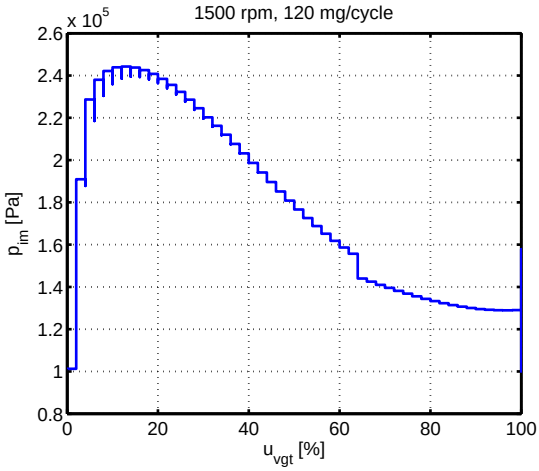

Figure 6.20. Stationary points collected in simulation, showing the intake manifold pressures that are possible to reach for engine speed 1500 rpm and 120 mg fuel/cycle injected. The maximum pressure is about 2.4 *bar* and the minimum when $u_{vgt} > u_{vgt}^{sgn}$ is about 1.3 *bar*.

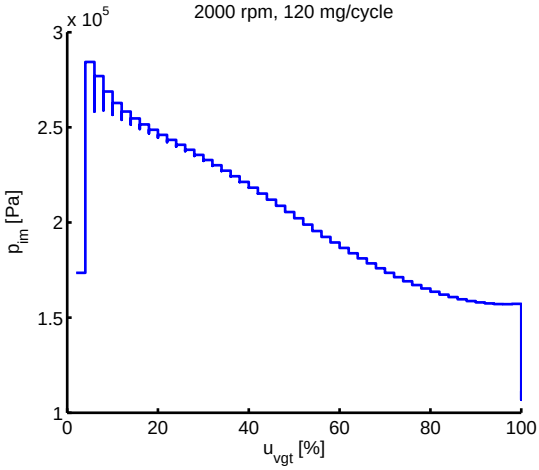

Figure 6.21. Stationary points collected in simulation, showing the intake manifold pressures that are possible to reach for engine speed 2000 rpm and 120 mg fuel/cycle injected. The maximum pressure is about 2.8 *bar* and the minimum when $u_{vgt} > u_{vgt}^{sgn}$ is about 1.7 *bar*.

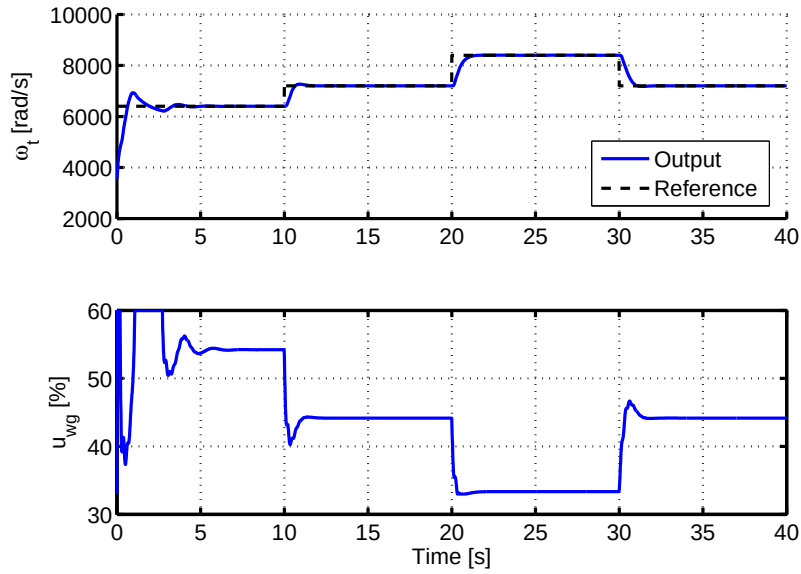

Figure 6.22. The figure shows how the controller manages to follow steps in reference signal. The reference signal goes from 6400 to 8400 rad/s. An increasing wastegate signal gives a greater wastegate area, which leads to a decreased turbine flow. The model controller reaches the goal of a time constant below 4 s with small overshoots. The control signal is not saturated during the simulation. Enginge speed is 2000 rpm and 120 mg fuel/cycle is injected.

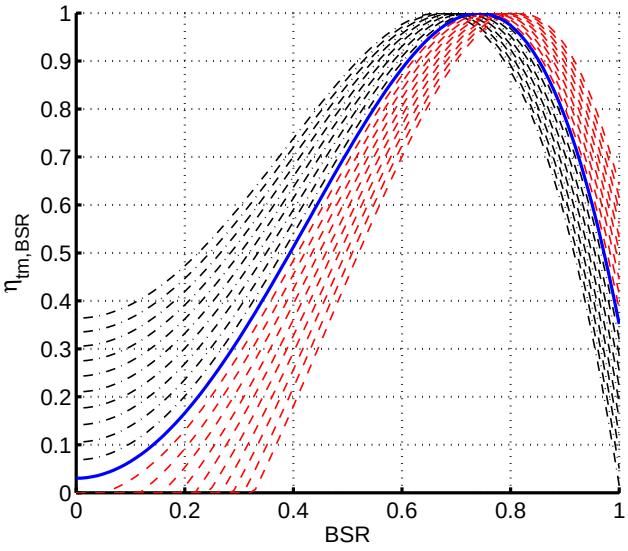

Figure 6.23. The figure shows $\eta_{tm,BSR}$ as a function of BSR with modeling errors in the parameter BSR_{opt}. The blue solid line corresponds to the optimized parameter value, the red dashed lines corresponds to positive modeling errors and the black dash-dotted lines correspond to negative modeling errors.

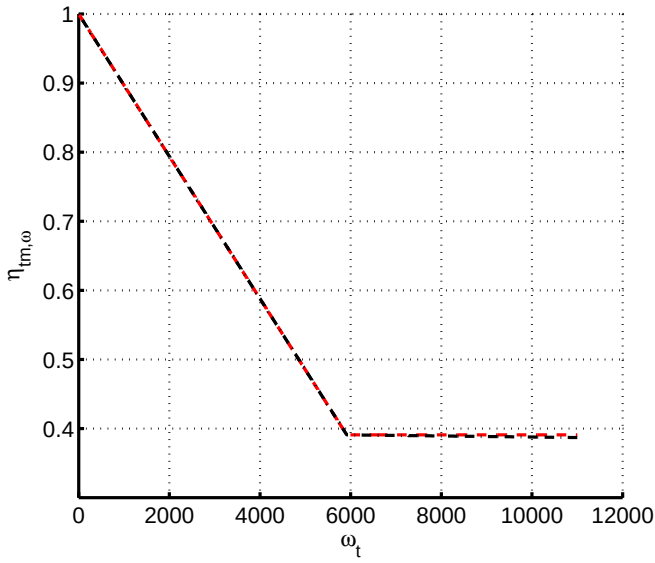

Figure 6.24. The figure shows $\eta_{tm,\omega}$ as a function of ω_t. The black dash-dotted line shows the original model and the red dashed line shows the model with $b_{\omega t2} = 0$. The difference is around 1 % for very high turbocharger speeds and much smaller for medium and low speeds.

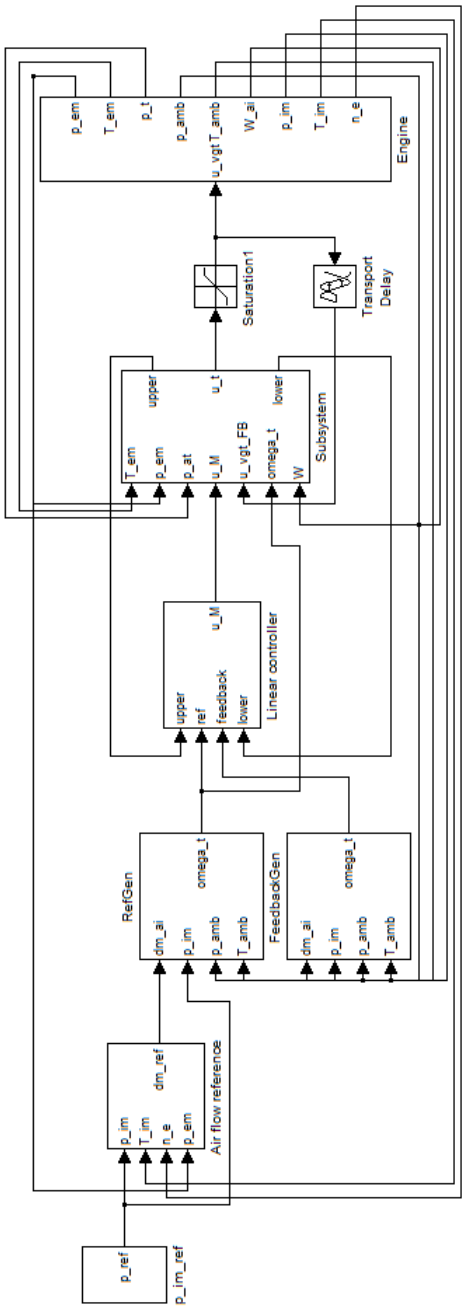

Figure 6.25. Simulink controller structure for simulation. From left to right: reference values in p_{im} and $\dot{m}_{ai}$, which is calculated from a volumetric efficiency based engine intake flow model, is fed to the compressor map based model RefGen. RefGen transforms these signals to reference value in ω_t, which is fed to the linear PIFF-controller. The PIFF-controller produces an output, u_M, which is transformed to the control signal u_t. In the engine model, there is a turbine sub-model, controlled by u_t, which produces turbine power, that is driving the compressor and intake air is compressed. The intake manifold pressure is measured and fed back to the compressor map based model to create a feedback in ω_t.

Chapter 7

Conclusions and future work

In this chapter, a brief sum-up of the results is given, as well as some ideas for future work. A model of a wastegated turbine is developed as well as a model-based control algorithm. The control algorithm was developed for the VGT first, and then the same approach was used for the wastegated turbocharger. To control the wastegate with the same algorithm as the VGT, an inverse of the developed static wastegate model is used.

The expected results are reviewed as follows. The control algorithm is not ready for use in test cell yet, but still needs some testing and evaluation on what complementary controllers have to be run in order to fulfil control objectives that were out of the scope of this project. The proposed control algorithm is developed the same way for wastegated SI engine and CI engine with VGT. The wastegate model has an absolute relative error of 3.6 % for the total flow, $\dot{m}_t$, and 7.4 % for the turbine efficiency, η_{tm}. The states n_t, p_{im}, $\dot{m}_{ei}$, x_{egr}, λ_O can not be evaluated since the engine model is not validated with the wastegated turbine. The transient behaviour in produced torque can be evaluated against step responses in intake manifold pressure, p_{im}. It is shown that the step responses in p_{im} are fast, with a rise time of around 1 s for a step with amplitude 1 bar. Common time constants for the pressure build-up are usually around 4 s, but for larger steps. It is also shown that fast steps can be made with overshoots smaller than the requested 5 %.

It would be interesting to further analyse how to predict the sign reversal point u_{vgt}^{sgn}, to be able to switch between the controllers used on each side of this point.

An opportunity for improvment of the model for the mass flow through the wastegate is to find an expression for the wastegate area that explicitly depends on the expansion ratio.

Bibliography

[1] P. Andersson, Air Charge Estimation in Turbocharged Spark Ignition Engines, *PhD Thesis,* Linköpings Universitet, 2004

[2] L. Eriksson, L. Nielsen, Modeling and Control of Engines and Drivelines, *Vehicular Systems, ISY*, Linköping Institute of Technology, 2010

[3] L. Eriksson, Modeling and control of turbocharged SI and DI engines, *Oil & Gas Science and Technology - Rev. IFP,* Vol. 62, No. 4, pp. 523-538, 2007

[4] T. Glad, L. Ljung, Reglerteknik, grundläggande teori, *Studentlitteratur, 4:th edition*, 2006

[5] L. Harnefors, J. Holmberg, J. Lundqvist, Signaler och system med tillämpningar, *Liber, 1:st edition*, 2004

[6] M. Jankovic, M. Jankovic, I. Kolmanovsky, Constructive Lyapunov Control Design for Turbocharged Diesel Engines, *IEEE Transactions on Control Systems Technology,* Vol. 8, No. 2, pp. 288-299, 2000

[7] M. Jung, K. Glover, U. Christen, Comparison of uncertainty parameterisations for H_∞ robust control of turbocharged diesel engines, *Control Engineering Practice,* Vol. 13, pp. 15-25, 2005

[8] M. Jung, Mean-Value Modelling and Robust Control of the Airpath of a Turbocharged Diesel Engine *PhD thesis,* University of Cambridge, 2003

[9] A. Karnik, J. Buckland, J. Freudenberg, Electronic Throttle and Wastegate Control for Turbocharged Gasoline Engines *2005 American Control Conference,* June 8-10, 2005. Portland, OR, USA

[10] D. Khiar, J. Lauber, T.M. Guerra, T. Floquet, Y. Chamaillard, G. Colin, Nonlinear modelling and control approach for a turbocharged SI engine, *IEEE Industrial Electronics,* IECON 2006 - 32nd annual conference, pp. 325-330, 2006

[11] P. Moraal, I. Kolmanovsky, Turbocharger Modeling for Automotive Control Applications, *SAE Technical Paper Series 1999-01-0908*, International Congress and exposition Detroit, 1999

[12] M. van Nieuwstadt, P. Moraal, I. Kolmanovsky, A. Stefanopoulou, P. Wood, M. Criddle, Decentralized and Multivariable Designs for EGR-VGT Control of A Diesel Engine *IFAC Workshop, Advances in Automotive Control,* 1998

[13] R. Rajamani, Control of a variable-geometry turbocharged and wastegated diesel engine *Proceedings of the I MECH E, Journal of Automobile Engineering*, Vol. 219, part D, 2005

[14] A. Shamdani, A. Shamekhi, M. Ziabasharhagh, C. Aghanajafi, Air-to-Fuel Ratio Control of a Turbocharged Diesel Engine Equipped with EGR using Fuzzy Logic Controller, *SAE Technical paper number 2007-01-0976*, 2007

[15] A. Stefanopoulou, I. Kolmanovsky, J. Freudenberg, Control of Variable Geometry Turbocharged Diesel Engines for Reduced Emissions, *IEEE Transactions on Control Systems Technology,* Vol. 8, No. 4, 2000

[16] J. Wahlström, Control of EGR and VGT for emission control and pumping work minimization in diesel engines, *Licentiate Thesis No. 1271,* Linköpings Universitet, 2006

[17] J. Wahlström, L. Eriksson, L. Nielsen, EGR-VGT Control and Tuning for Pumping Work Minimization and Emission Control *IEEE Transactions on Control Systems Technology,* Vol. 18, No. 4, 2010

[18] J. Wahlström, L. Eriksson, Modelling diesel engines with a variable-geometry turbocharger and exhaust gas recirculation by optimization of model parameters for capturing non-linear system dynamics, *Proceedings of the Institution of Mechanical Engineers, Part D, Journal of Automobile Engineering*, Vol. 225, No. 7, pp. 960-986, 2011

[19] J. Wahlström, L. Eriksson, Non-linear Compensator for handling non-linear Effects in EGR VGT Diesel Engines, *Technical Report No. LiTH-ISY-R-2897,* Linköpings Universitet, 2009

[20] J. Wahlström, L. Eriksson, Nonlinear EGR and VGT Control with Integral Action for Diesel Engines. *In: IFAC Workshop on Engine and Powertrain Control, Simulation and Modeling,* Paris, France, 2009

[21] J. Wahlström, L. Eriksson, Robust Nonlinear EGR and VGT Control with Integral Action for Diesel Engines *IFAC World Congress*, Seoul, Korea, 2008

[22] J. Wahlström, L. Eriksson, L. Nielsen, System analysis of a Diesel Engine with VGT and EGR, *Technical Report No. LiTH-R-2881,* Linköpings Universitet, 2009